

THIS PAGE INTENTIONALLY LEFT BLANK

AN ABSTRACT OF THE THESIS OF

Anthony M. Rikli for the degree of Master of Science in Civil Engineering presented on May 25, 2011.

Title: Evaluation of Straw Wattle Placement and Surficial Slope Stability

Abstract approved:

Michael J. Olsen

Straw wattles are common erosion control devices used to trap sediment. This thesis studies the relationship of straw wattles on slope stability through a case study demonstrating their use on steep slopes (1.5H:1V) for the US20 highway realignment project. Several surficial slope failures have occurred on these fill slopes, often bracketed by straw wattles, which were hypothesized to contribute to the slope failures. To date, little is known about straw wattle placement and its effect on surficial slope stability. Prior studies have evaluated slope stability against slope height, slope angle, vegetation, rainfall, and other variables but have not assessed the influence of straw wattle placement on surficial stability.

Several laboratory tests were performed to characterize the fill soil and the straw wattles for numerical modeling and evaluation. Straw wattles were shown to quickly absorb a substantial amount of water (a water content of 400% within 15 minutes) and require a substantial amount of time to dry (several days at high temperatures). Several

modeling scenarios were run (varying the slope angle, slope height, straw wattle spacing and climate condition) to determine the overall effect of straw wattles on deep and surficial slope stability. Overall, straw wattles were shown to have no significant effect on surficial slope stability, particularly compared to modeling uncertainty and soil variability. Of the 366 models run, 26% showed a change in factor of safety (0.006 on average) against surficial slope failure when straw wattle spacing was increased. Over half of the 26% showed a decrease in factor of safety.

Other influencing factors such as slope angle, ground water elevation and environmental conditions have a much more significant impact on slope stability. The slopes themselves were found to have a low factor of safety (≤ 1 , at the limit of equilibrium) against surficial slope failures and a reasonable factor of safety (> 1.5) against deeper failures, regardless of straw wattle spacing. Investigations using 3D laser scanning verified that straw wattles were installed along the same slope contours, therefore, not allowing water to pond behind the straw wattle and decrease the factor of safety against surficial slope failure.

©Copyright by Anthony M. Rikli

May 25, 2011

All Rights Reserved

Evaluation of Straw Wattle Placement and Surficial Slope Stability

by

Anthony M. Rikli

A THESIS

submitted to

Oregon State University

in partial fulfillment of
the requirements for the
degree of

Master of Science

Presented May 25, 2011
Commencement June 2011

Master of Science thesis of Anthony M. Rikli

presented on May 25, 2011.

APPROVED:

Major Professor, representing Civil Engineering

Head of the School of Civil and Construction Engineering

Dean of the Graduate School

I understand that my thesis will become part of the permanent collection of Oregon State University libraries. My signature below authorizes release of my thesis to any reader upon request.

Anthony M. Rikli, Author

ACKNOWLEDGEMENTS

This thesis could not be completed without the immense help of many people. I would like to thank Granite Construction for providing funding to analyze the relationship of surficial slope failures and straw wattle placement. I would also like to thank Craig Gehling and Torger Torgersen of Granite Construction for their help in gathering information about the project as well as help with moving equipment for LIDAR photos around the site. Kevin Severson was also an immense help with starting the project and getting me acquainted with the US 20 project.

Dr. Jerry Yamamuro and Dr. David Sillars developed much of the original concepts for the project. Dr. Sillars also gave much advice and guidance in completing this work as well as throughout the thesis' project life. I would also like to thank Dr. Kellogg and Dr. Stuedlein for their time and work in editing this thesis and accepting the invitation to be a part of my graduation committee.

I would like to thank my advisor, Michael Olsen, for his incredible help, advice and support throughout this project and sacrificing many hours going over calculations and thesis drafts. Evon Silvia and Shawn Butcher also assisted with LiDAR scans out on the job site as well as with organizing and rendering data gathered.

I would like to thank the geotech office at OSU as well as the community that was built over the past year. Being a part of this group made completing this thesis that much easier.

Most importantly, I would like to thank my wife and family for their incredible support throughout this thesis production and my educational career.

CONTRIBUTION OF AUTHORS

Drs. Olsen and Sillars assisted in the development of this thesis and will be co-authors on future publications resulting from this work.

TABLE OF CONTENTS

	<u>Page</u>
1 Introduction	2
1.1 Overview	3
1.1.1 Thesis Outline and Objectives.....	4
1.2 Slope Stability Failure Types	5
1.3 Evaluating Surficial Slope Stability	6
1.4 Slope Gradient, Height and Shape	8
1.4.1 Rainfall	9
1.4.2 Soil Hydraulic Conductivity.....	10
1.4.3 Vegetation	11
1.4.4 Cohesive Soil Shrinkage	13
1.5 Site Description	13
1.5.1 Geography/Geology	14
2 Straw Wattles	16
2.1 Overview	17
2.2 Common Erosion Control Devices (ECDs)	17
2.3 Straw Wattle Studies	18
2.4 Straw Wattle Testing.....	21
2.5 Straw Wattle Results	22
3 LiDAR Analysis.....	25
3.1 Overview	26
3.2 Straw Wattle Installation.....	26

TABLE OF CONTENTS (Continued)

	<u>Page</u>
3.3 LiDAR Overview	27
3.3.1 Purpose	28
3.4 Observations.....	28
3.5 Conclusion.....	28
4 Soil Testing.....	31
4.1 Overview	32
4.2 Testing Overview	32
4.2.1 Grain Size Distribution Analysis.....	33
4.2.2 Atterberg Limits	34
4.2.3 Standard and Modified Compaction Test.....	37
4.2.4 Shear Strength Testing	41
4.2.5 Hydraulic Conductivity Testing	52
4.2.6 Swell Testing.....	53
4.3 Testing Program Results	54
4.3.1 Soil Classification and Atterberg Limits.....	54
4.3.2 Standard and Modified Compaction Test.....	56
4.3.3 Consolidated – Undrained Triaxial Test	58
4.3.4 Hydraulic Conductivity	59
4.3.5 Swell Test.....	60
5 Numerical Slope Stability Modeling.....	61
5.1 Limit Equilibrium Slope Stability Modeling	62
5.1.1 Overview	62
5.2 Limit Equilibrium Slope Stability Modeling Procedure	63
5.3 Seepage and Climate Modeling.....	65

TABLE OF CONTENTS (Continued)

	<u>Page</u>
5.3.1 Overview	65
5.3.2 Seepage and Climate Modeling Procedure	66
5.4 Modeling Results.....	67
5.4.1 Surficial Slope Failure Formation.....	67
5.4.2 Impact of Straw Wattles.....	67
5.4.3 Impact of Groundwater	72
5.4.4 Impact of Climate.....	75
6 Conclusions and Recommendations.....	77
6.1 Conclusions	78
6.2 Recommendations	78
6.3 Future Evaluation	81
Bibliography	83
Appendices	88
Appendix A Site and Boring Properties	89
Appendix B Lab Test Data.....	93
Appendix CD Slope/W and Vadose/W Modeling Results.....	105

LIST OF FIGURES

<u>Figure</u>	<u>Page</u>
1. Surficial slope failures and straw wattles on Fill 7	3
2. Mohr-Coulomb failure envelope.....	7
3. Conceptual fill slope	19
4. Straw wattle water content over time.....	23
5. Drying straw wattle weight over time.....	24
6. Example of straw wattle placement on-site	26
7. DTM of LiDAR scan of straw wattle elevations on slope.....	29
8. DTM of LiDAR scan of fill slope with constant straw wattle elevation	29
9. LiDAR survey of slope failure on US20PME	30
10. Atterberg Limits and soil states (Modified from Ecoles Des Ponts, 2010)	35
11. Casagrande device, grooving tool, and plastic limit equipment	37
12. General compaction test procedure.....	40
13. Example of standard compaction test results.....	41
14. Triaxial and cell apparatus	44
15. 144kPa consolidation curve	49
16. Failed soil in consolidated undrained triaxial test.....	51
17. A soil sample at failure after a CU triaxial compression test	52
18. Plasticity chart for Fill 6, 8, and 10.....	55
19. Grain size distribution plot for Fills 6, 8, 10.....	56
20. Standard and Modified Compaction Test Results	57

LIST OF FIGURES (Continued)

<u>Figure</u>	<u>Page</u>
21. Approximate Mohr-Coulomb failure envelope from CU test (Fill 6)	59
22. Slope/W slope model 1.5H:1V slope ratio	64
23. Factor of safety map against slope failure	69
24. Factor of safety map for scenario with no straw wattles. Shades toward the surface represent decreased stability; shades toward the bottom represent increased stability.....	71
25. Factor of safety map for scenario with 25 ft straw wattle spacing. Note that the darker shade at the bottom disappears at the bottom of the slope compared to Figure 24.....	71
26. Failure circle with 25ft straw wattle spacing, 3m high water table	74
27. Failure circle with 75 ft straw wattle spacing, 3 m high water table	74
28. Failure circle with no straw wattles, 3m high water table	75
29. January 2008 rainfall.....	76
30. Slope /W with Vadose/W results	76
31. January 2008 temperature	76

LIST OF TABLES

<u>Table</u>	<u>Page</u>
1. Typical sieve openings.....	33
2. Compaction methods for standard compaction tests	39
3. Compaction methods for modified compaction tests.....	39
4. Test result summary and soil classification	55
5. Standard compaction test data and comparison	57
6. Slope/W factors of safety for 30 and 40 meter tall fills without Vadose/W.....	68
7. Factors of safety from critical slip surfaces with varying groundwater levels for 30m high fill with 1.5H:1V slope	73

LIST OF APPENDIX TABLES

<u>Table</u>	<u>Page</u>
A- 1. 50G site and boring properties (Natural Resources Conservation Service)	90
B- 1. Sieve analysis data for Fill 6	94
B- 2. Sieve analysis data for Fill 8	94
B- 3. Sieve analysis data for Fill 10	95
B- 4. Fill 6 liquid limit, plastic limit and plasticity index data	95
B- 5. Fill 8 liquid limit, plastic limit and plasticity index data	96
B- 6. Fill 10 liquid limit, plastic limit and plasticity index data	96
B- 7. Standard compaction data for Fill 6	97
B- 8. Standard compaction data for Fill 8	97
B- 9. Standard compaction data for Fill 10	98
B- 10. Modified compaction data for Fill 6	99
B- 11. 36kPa CU triaxial test data	99
B- 12. 72kPa CU triaxial test data	100
B- 13. 144kPA CU triaxial test data	100
B- 14. Fill 6 consolidation data for hydraulic conductivity	101
B- 15. Fill 8 consolidation data for hydraulic conductivity	102
B- 16. Fill 10 consolidation data for hydraulic conductivity	103
B- 17. Fill 10 1D Swell Test	104
B- 18. Fill 6 Free Swell Test	104
CD- 1. Factor of safety results for 30 m high fill at 1H:1V slope	106

LIST OF APPENDIX TABLES (Continued)

<u>Table</u>	<u>Page</u>
CD- 2. Factor of safety results for 30 m high fill at 1.5H:1V slope	107
CD- 3. Factor of safety results for 30 m high fill at 2H:1V slope	108
CD- 4. Factor of safety results for 40 m high fill at 1H:1V slope	109
CD- 5. Factor of safety results for 40 m high fill at 1.5H:1V slope	110
CD- 6. Factor of safety results for 40 m high fill at 2H:1V slope	111

LIST OF SYMBOLS AND ABBREVIATIONS

Symbol/Abbreviation	Description
ASTM	American Society for Testing And Materials
BMP	Best Management Practice
CD	Consolidated Drained
CU	Consolidated Undrained
DOGAMI	Oregon Department of Geology and Mineral Industries
DOT	Department of Transportation
ECD	Erosion Control Device
LI	Liquidity Index
LiDAR	Light Detection And Ranging
LL	Liquid Limit
LVDT	Linear Variable Displacement Transducer
NCDC	National Climatic Data Center
NOAA	National Oceanic and Atmospheric Administration
ODOT	Oregon Department of Transportation
PI	Plastic Index
PL	Plastic Limit
PWP	Pore Water Pressure
QC	Quality Control
US20PME	US 20 Pioneer Mountain to Eddyville Project
USC	Unified Soil Classification
UU	Unconsolidated Undrained
VCD	Volume Change Device
c, c'	Cohesion intercept (Undrained, drained)
D	Seepage depth
d_0	Displacement at Zero Percent Consolidation
d_{50}	Displacement at Fifty Percent Consolidation
d_{100}	Displacement at One Hundred Percent Consolidation
FS	Factor of Safety
H	Fill Height
I_{min}	Minimum rainfall intensity equal to the infiltration rate in a soil
k_{lim}	Critical Hydraulic Conductivity
S	Straw Wattle Spacing
s	Wetting Front Capillary Suction
t_0	Time at Zero Percent Consolidation
t_{50}	Time at Fifty Percent Consolidation
t_{100}	Time At One Hundred Percent Consolidation
WC	Water Content of Soil
z_w	Depth of saturation in soil

LIST OF GREEK SYMBOLS

Symbol/Abbreviation	Description
α	Slope inclination angle
$\dot{\epsilon}$	Strain Rate
γ_t	Total density of soil
	Density of water
ϕ, ϕ'	Friction angle (total, effective)
σ'_{ff}	Effective Normal Stress at Failure on the Failure Plane
τ'_{ff}	Effective Shear Stress at Failure on the Failure Plane

Evaluation of Straw Wattle Placement and Surficial Slope Stability

Chapter 1: Introduction

1.1 Overview

The US20: Pioneer Mountain to Eddyville Project (US20PME) is a design-build project undertaken by Granite Construction in 2006. Located within the coastal mountain range near Eddyville, Oregon, the site experiences high amounts of rainfall (typically 74.5 in/year (189 cm/year)). Approximately 95% of the rainfall occurs during the wet season (October 1st to May 31st). Before this period, after each fill is constructed for the project, straw wattles are installed level with slope contours at 25 foot spacings to trap sediment and prevent it from entering nearby waterways. During the wet season, however, several surficial slope failures were observed; many of which were bracketed by the straw wattles, as shown in Figure 1.

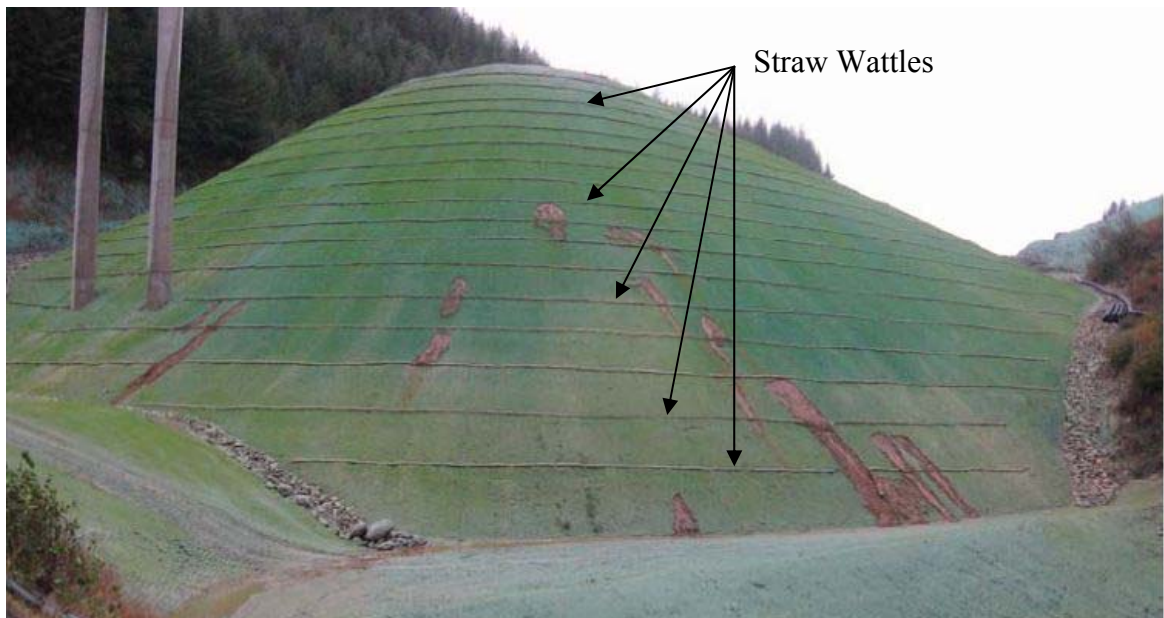


Figure 1. Surficial slope failures and straw wattles on Fill 7

Although surficial failures are mainly ignored in design and often remediated in construction due to their infrequency and size, at US20PME, these have occurred often

enough to be costly to repair and cause some alarm. Currently, the failed slope sections are temporarily covered with plastic sheeting to prevent sediment transfer to nearby rivers. The fills are, then, remediated by removing the sloughed material and rebuilding the slope. The economic and environmental penalties of these failures can continue past construction and require ongoing maintenance.

If the failures do occur because of straw wattle placement, these problems could continue in the future. Therefore, more research is needed to understand the effect of straw wattles on both surficial slope stability and their effect on potential failures deeper in the slope. Hypotheses considered were:

1. Do straw wattles back up water on the slope, due to discrepancies in installment elevation, causing increased load and failure?
2. Do straw wattles add weight to the embankment slope, causing a surficial failure?
3. Do straw wattles prevent deeper failures from occurring?

1.1.1 Thesis Outline and Objectives

To evaluate these hypotheses, a work plan was created with the following goals:

- Gather literature concerning surficial failures and slope stability (Chapter 1).
- Characterize the site environment and geological area (Chapter 1).
- Collect literature on straw wattles; assess how they were installed on-site and their properties (Chapter 2).

- Analyze general parameters of an embankment slope and verify level contour straw wattle installation using Light Detection and Ranging equipment (LiDAR) (Chapter 3).
- Complete soil testing of on-site fill samples to find the soil properties of the fill embankments (Chapter 4).
- Model slope stability using the soil and straw wattle properties (Chapter 5).
- Determine any relationships between straw wattles and slope failures (Chapter 6).
- Provide recommendations regarding the observed surficial slope failures (Chapter 6).

1.2 Slope Stability Failure Types#

According to Cruden and Varnes (1996), the mechanisms of slope failures can be classified as falls, topples, slides, lateral spreads, flows, or a combination. Of the many different ways landslides can occur, each is designated as one of two types: shallow and deep.

Surficial slope failures are a subcategory of shallow slope failures, which generally range in depth from 0 to 1.2 ft (0 to 0.37 m) (Evans, 1972). These slides occur parallel to the ground surface along either bedrock or a low permeability layer (Sidle & Ochiai, 2006). . Surficial failures tend to have a length greater than their width, have depth to height ratios < 0.1 (Sidle & Ochiai, 2006), and mainly occur on slopes that are linear or concave upward.

Deep failures, in contrast, generally occur at depths greater than 16.4 feet (5 m) and often have a material composition of weathered bedrock (Sidle & Ochiai, 2006). These failures are much larger in size when compared to what was observed on-site and, as such, this discussion will focus on surficial slope failures.

1.3 Evaluating Surficial Slope Stability

Slope stability is determined by the ratio of forces driving failure and forces resisting failure. The soil's shear strength is its capacity to resist failure and is described by the friction angle (ϕ') and cohesion (c') of the soil in Mohr-Coulomb Theory. These parameters are shown in a Mohr-Coulomb diagram shown in Figure 2. The force driving failure is the weight of the soil mass and the load applied to it. Theoretically, the points on the circles (Figure 2) that are tangent to the Mohr-Coulomb failure envelope represent the stress conditions at which the driving forces have become greater than the resisting forces. This is considered a strength failure in the soil. Notice that this failure envelope assumes a soil's strength fails linearly with increasing stress with a cohesion intercept (c') at zero effective normal stress. In reality, however, this cohesion is not fully mobilized at low stresses. Therefore a lower intercept is produced, creating a curved, rather than linear, strength failure envelope (Holtz, Kovacs, and Sheahan, 2010).

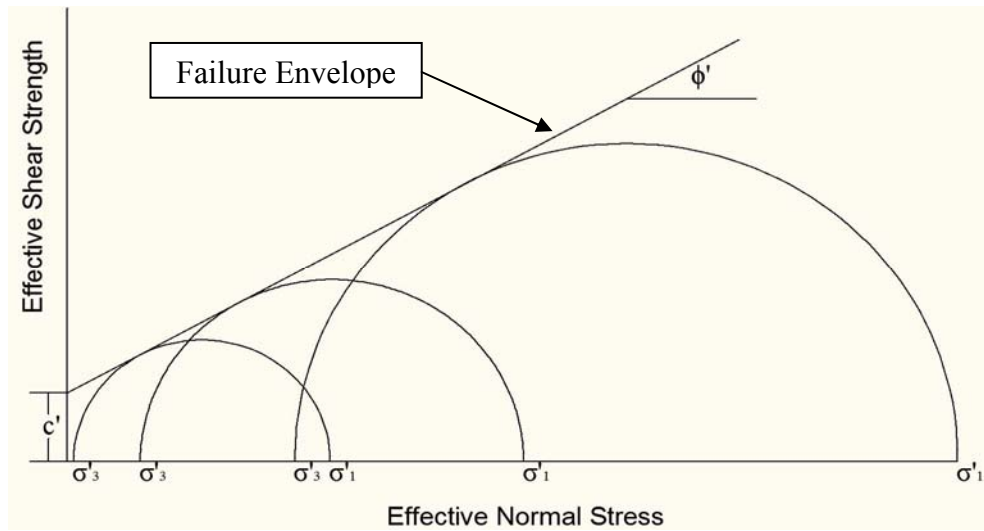


Figure 2. Mohr-Coulomb failure envelope

The ratio of these driving and resisting forces is considered the factor of safety (FS) against slope failure. If the factor of safety is greater than one (i.e. resisting forces are greater than driving forces), the slope is considered stable. If, however, the factor of safety is less than one (resisting forces are less than driving forces), the slope is considered unstable. Using infinite slope analysis, Equation 1 (Lambe and Whitman 1969) can be used to calculate this factor of safety for surficial failures resulting from seepage parallel to the slope face:

$$FS = \frac{c' + (\gamma_t - \gamma_w)D \cos^2(\alpha) \tan(\phi')}{\gamma_t D \sin(\alpha) \cos(\alpha)} \quad (\text{Eq. 1})$$

where:

FS = factor of safety,

c' = cohesion intercept,

γ_t = total density of soil,

γ_w = density of water,

D = seepage depth,

ϕ' = effective friction angle,

α = slope inclination.

Day (1994) analyzed the surficial stability of compacted clay and found that consolidated undrained (CU) triaxial tests used to evaluate overall slope stability tend to over-estimate cohesion in clays, even at relatively low effective stresses. By using Equation 1, Day determined also that the factor of safety can be overestimated when using these cohesion values. Day recommends an unconfined submerged triaxial test be completed on the soil for determining strength parameters (especially cohesion), which results in a factor of safety value closely modeling in-field conditions.

1.4 Slope Gradient, Height and Shape

In addition to the soil's strength, the inclination angle (α) can have a significant effect on slope stability (Sidle & Ochiai, 2006; Rahardjo, Ong, Rezaur, & Leong, 2007). Rahardjo et. al. (2007) found that with every increase of 1 degree the initial factor of safety reduces by 2.32% for a given soil material.

Fill height can also result in a reduction in factor of safety against surficial failure. The initial factor of safety decreases exponentially as the slope height increases, but, a slope height of 16.4 feet (5 m) remains stable regardless (Rahardjo, et. al., 2007).

Slope shape also has a considerable effect on its stability. There are three principal types of slope shapes: divergent, planar, and convergent. Of the three types, divergent is the most stable, as characterized by Sidle & Ochiai (2006). With other site

variables constant, divergent landforms are generally most stable in steep terrain, followed by planar hillslope segments and convergent or concave hillslopes (Sidle & Ochiai, 2006). Furthermore, divergent landforms allow subsurface and surface waters to evaporate, reducing pore pressures throughout the slope. In contrast, convergent slopes create rapid pore water pressure increases during storms or periods of snowmelt (Sidle, 1984; Fernandes, Netto, & Lacerda, 1994; Montgomery et al., 1997; Tsuboyama et al. 2000).

1.4.1 Rainfall

Significant rainfall can also cause slope instability due to an increase in seepage forces and pore water pressures. Rainfall characteristics affecting stability include: (1) total amount of rainfall, (2) short-term intensity, (3) antecedent storm precipitation, and (4) storm duration. Examining the four factors, Sidle & Ochiai (2006) show that the short term intensity of rainfall, coupled with antecedent storm precipitation and storm duration, can cause simulated landslides on a hillslope.

In Oregon, the Department of Geology and Mineral Studies (DOGAMI) studied this relationship from west of the Cascades to the ocean beaches. Oregon experienced unusual amounts of rainfall during four storms from February 1996 to January 1997. During this same time frame, numerous debris flows were recorded in the area described above. Thomas Wiley, of DOGAMI, gathered rainfall data from this period from various weather stations at these failure locations and analyzed it against mean December rainfall and the mean annual precipitation. The mean December rainfall was used because

December shows the most rainfall in the year, according to many National Oceanic and Atmospheric Administration (NOAA) weather stations (Wiley, 2000).

Wiley found that the data suggested slides will occur in western Oregon when 8 inches (20 cm) of rain has fallen since the end of September 1996 and 24-hour rainfall exceeds 40 percent of mean December rainfall (Wiley, 2000). Rainfall data for Eddyville was not available from DOGAMI's research. However, surrounding weather stations, using data gathered by the National Climatic Data Center (NCDC) and the NOAA, suggest that the 40 percent of mean December 1996 rainfall ranged from 4.47 to 4.98 inches (11.4 to 12.6 cm) (Wiley, 2000). Following Wiley's methodology for the US20PME project site, we can estimate a landslide will occur if 4 to 6 inches (10 to 15 cm) falls on a natural fill slope if, as stated earlier, 8 inches (20 cm) of rainfall has fallen since the month of September.

1.4.2 Soil Hydraulic Conductivity

Soil permeability is also an important consideration for slope stability. Pradel and Raad (1993) found that soils with a low critical hydraulic conductivity threshold ($k_{lim} < 10^{-4}$ cm/sec) for the Southern California area, typically fine-grained soils, are more prone to saturation. Soils with a permeability greater than k_{lim} (typically sands and gravels) will not become saturated. If full saturation is achieved, a shear failure plane develops parallel to the slope surface due to a loss of adhesion between soil particles. This reduces the resisting force greatly and therefore decreases the factor of safety against failure. The critical hydraulic conductivity threshold is a function of rainfall intensity and duration (Pradel & Raad, 1993).

$$k_{\text{lim}} = I_{\text{min}} \left(\frac{z_w}{z_w + s} \right) \quad (\text{Eq. 2})$$

where:

I_{min} = minimum precipitation intensity for saturation

z_w = depth of saturation

s = wetting front capillary suction

It should be noted that I_{min} must be greater than or equal to the infiltration rate of the soil for saturation to occur. For Oregon, I_{min} may be larger than for Southern California because of substantially more precipitation, and thus, k_{lim} may be larger. Cho and Lee (2002) modified the formulation developed by Pradel and Raad (1993) and analyzed the decrease in factor of safety with continual rainfall.

Rahardjo et. al. (2007) determined that a saturated homogeneous soil slope with a hydraulic conductivity less than $3.28\text{E-}6$ feet/sec (10^{-6} m/sec) is generally safe from failure caused by short-duration rainfalls regardless of intensity. Soils with a larger hydraulic conductivity are susceptible to failure, most of which are due to ground water table mounding. For lower conductivities, the soil's matric suction above the water surface can be important and should be considered (Rahardjo et. al., 2007).

1.4.3 Vegetation

Vegetation, grasses and trees in particular, can help slope stability by evapotranspiration (Bishop & Stevens, 1964) and soil reinforcement to the soil (Sidle & Ochiai, 2006). Because of differences in temperature, vegetation can evaporate the soil's moisture into the air, increasing the soil's adhesion and friction angle, which can, overall,

increase the soil's strength. This benefit mostly occurs for shallow depths, as root distribution is concentrated within 1 m of the ground surface for trees (Greenwood et. al., 2004) and much shallower for grasses.

If vegetation is removed, this action can have adverse effects. Many studies have found a 2 to 10 fold increase in rates of soil erosion 3 to 15 years after timber was harvested from soil slopes (Bishop & Stevens, 1964; Endo & Tsuruta, 1968; Fujiwara, 1970; Swanson & Dyrness, 1975). This is most likely due to the introduction of rainfall on these less forested slopes and can be inferred that the use of vegetation increases slope stability.

Gray & Sotir (1992) show that living woody plant material provided quick reinforcement for the slope and encouraged more plants to grow. Also, these roots are believed to reduce pore pressures by intercepting rainfall and by evapo-transpiration (Wu, Riestenberg, & Flege, 1994). Van De Wiel and Darby (2007) also found that, when analyzing stability of riverbanks in relation to root reinforcement and tree weight surcharge, woody vegetation can influence the bank's stability when it is located either at the bank toe or at the intersection of the failure plane and the floodplain.

Day (1993) compiled a case study discussing the relationship between surficial slope stability and vegetation in southern California. In this study, Day performed several direct shear tests and CU triaxial compression tests on remolded samples from compacted fills where surficial slope failures were observed. To model field conditions, Day incorporated root development into his direct shear tests by tending and growing grass into the tested sample for a period of five weeks prior to testing. The grass was then shorn

and the soil was tested. These tests were then compared with tests done on organic-free soils of the same composition.

From the results, Day saw that a failure plane had developed just below the grass roots and that the drained shear strength was much higher for root-reinforced samples (Day, 1993). Moreover, Day, using infinite slope analysis, found that the factor of safety on a non-root reinforced soil was almost halved if seepage parallel to the slope occurred.

1.4.4 Cohesive Soil Shrinkage

Cohesive soil shrinkage can also have an effect on slope stability. According to Rogers and Selby (1980), shrinkage can reduce slope stability by shortening the failure surface length where the shearing resistance is instigated. Also, as a result of the tension cracks formed from repeated expansion and contraction, precipitation can infiltrate the soil and seepage forces can develop within the soil due to high intensity storms.

1.5 Site Description

Given all these factors that can affect slope stability, more information is needed on the project case study and its environment. The US 20: Pioneer Mountain to Eddyville project straightens a section of US 20 ultimately making the highway three miles shorter and, by eliminating several turns and intercity travel, safer. Widening the highway will allow interstate trucks to use the route and more passing lanes will be available than previously (Yaquina River Constructors, 2008-2010).

The project site is located in a heavily wooded, predominantly Douglas Fir forest. From data gathered on-site and in surrounding areas, from 2006 to 2010, the average amount of rainfall during the wet months was 74.5 inches (179 cm) and temperature

ranged from 17 to 97 degrees Fahrenheit (-8 to 36 degrees Celsius). Mountain lions, elk and deer are present in and along the job site and have possibly destabilized the fill slopes.

The realignment project was designed to eliminate hairpin curves, railroad crossings, visual barriers for motorists, lower congestion and construct new bridges that follow current structural code. In doing so, the highway was straightened and various highway embankments were created using on-site soils. Where there were numerous no-passing zones before, the design allowed for two wide lanes of travel, wide shoulders and passing lanes (Yaquina River Constructors, 2008-2010).

1.5.1 Geography/Geology

The US 20: Pioneer Mountain to Eddyville project lies within the Tyee Formation, which is composed of sediments deposited on a rigid fore-arc block that were subsequently accreted during the upper Eocene and Oligocene period (Van de Water, Leavitt, Jull, Squire, & Testa, 2009). The sediments were tilted, folded and faulted resulting in flexure slip along bedding planes (Hammond, Meier, & Beckstrand, 2009). Subsequent uplift (Kelsey, Ticknor, Bockheim, & Mitchell, 1996) destabilized hillslopes and allowed landslides to develop with the onset of erosion and deepening of area drainages (Van de Water, Leavitt, Jull, Squire, & Testa, 2009).

This area includes rhythmic-bedded units of graded sandstone and siltstone and lateral continuity of these units. The Tyee formation also has graded beds that are poorly sorted with sharp soles containing directional features with preferred orientations (such as

groove casts and flute casts) with tabular siltstone clasts with pull-aparts (Snively, Wagner, & MacLeod, 1964).

The project site's natural topography typically ranges in slope ratios of 2.9H:1V to 1.6H:1V (19° to 31°) with elevations varying from 30 to 1800 feet (9 to 549 m) (National Resource Conservation Society, 2009). Also, much of the proposed roadway, lies within the 50 G outlined area, labeled as the Preacher – Bohannon – Slickrock complex. These areas characterize the average natural slope, geologic material, and environmental conditions that occur and these characteristics are shown in Table A-1 in Appendix A.

The highway embankments are constructed with material from the site, vary in height from 98 to 131 feet (30 to 40 m) and resemble planar slopes. On average, the slope inclines 1.5H:1V (33.7°), which is significantly steeper than the natural topography. Both heights and slope inclines were found using LiDAR, which will be discussed later. The fill embankments generally consist of material excavated from cut areas on-site, which consist of a matrix of sandstone and mudstone with some basalt gravel. These embankments are placed using haul trucks and compacted using sheep's foot rollers. According to Granite Construction's compaction quality control data for Fill 6, the average dry density is 94.1 lbs/ft³ (14.8 kN/m³) with an optimum moisture content of 24%. Fills 8 and 10 were compacted in a similar manner and it is assumed that both dry density and water content are comparable. Sufficient densities for compaction were specified using the standard compaction test.

Chapter 2: Straw Wattles

2.1 Overview

To understand the effect straw wattles have on surficial slope stability various tasks were completed. These include:

- Review of state specifications for straw wattles.
- Collection of literature on straw wattles, their uses, and their advantages and disadvantages on-site.
- Testing of straw wattles to gain their dry and saturated weight, and also drying time required to return to their dry weight.

2.2 Common Erosion Control Devices (ECDs)

In practice, there are various types of erosion control devices that many state departments of transportation (DOTs) use across the country. There are many ways to reduce the amount of sediment lost from the construction site (e.g. rip-rap, check dams, straw wattles). For example, plastic sheeting is used to increase slope protection and increase the protection of the slope toe. Sediment fences can be used to decrease the amount of soil leaving from the construction site and also to protect the water quality of nearby waterways. Herein, our focus will be concentrated on straw wattles and their use on the US 20: Pioneer Mountain to Eddyville project.

Straw wattles are a common erosion control device used by DOTs and contractors across the country. For the Maryland DOT, natural straw wattles are used to stabilize slopes and improve aesthetics by encouraging vegetation growth (Maryland Department of the Environment Water Management Administration, 1999). These wattles are composed of biodegradable materials such as coir fiber and commercially available in 16

to 18 inch diameter rolls (Maryland Department of the Environment Water Management Administration, 1999).

The Oregon Department of Transportation (ODOT) specifies straw wattles to be 8 to 10 inch (20 to 25 cm) in diameter size, have minimum strand thickness of 0.003 inch, a knot thickness of 1/16 inch, weight of 0.35 ounces per foot \pm 10% and made from 85% high density polyethylene, 14% ethyl vinyl acetate, and 1% color for UV inhibition (Oregon Department of Transportation, 2008). ODOT specifies that the straw provided should not be moldy, caked, decayed or of otherwise low quality and the straw is free of noxious weed seeds or plant parts and (Oregon Department of Transportation, 2008) has certified that the straw wattles installed at US20PME meet these specifications.

2.3 Straw Wattle Studies

Many straw wattle studies research the device's effectiveness in filtering runoff water on fill slopes. However, little, if any, information is known on the relationship between straw wattles and slope stability. The following section discusses straw wattles, their purpose concerning the US20PME project, and what has been found regarding their filtering effectiveness with varying environmental factors.

From earlier in this study, wattles were installed approximately 25 feet (7.6 m) apart from each other along the slope of the fill embankment. Also no vegetation was planted along the slope. However, once the slope was showing failure bracketing between the straw wattles, vegetation was placed on the slopes and the spacing between the wattles was widened to 75 feet. Figure 3 shows, conceptually, the main components of a fill slope in the US20PME project.

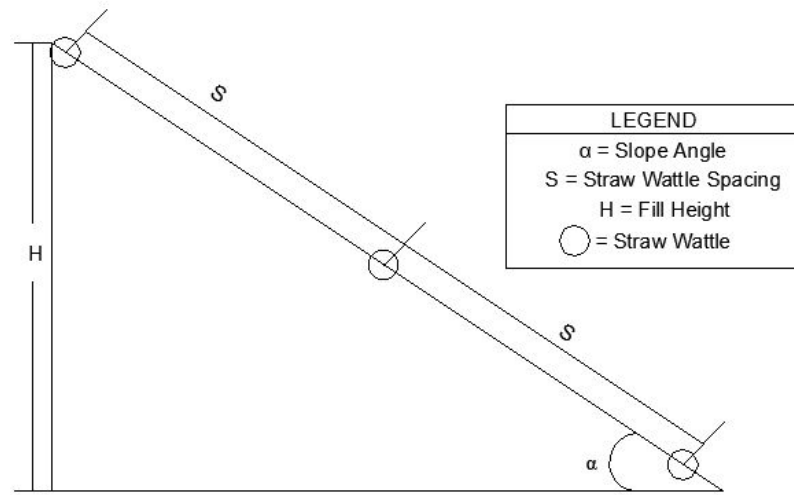


Figure 3. Conceptual fill slope

Kelsey, Johnson, and Vavra (2006) conducted a study of various erosion control devices and their performance during rainfall periods. In continuation of previous research (Kelsey, et. al., 2005), Kelsey et al. (2006) examined a 9 inch thick diameter straw wattle and a 12 inch thick diameter straw wattle including other various devices of erosion control. In their study, straw wattles were exposed to a 2.0 in/hr (5.1 cm/hr), a 4 in/hr (10.2 cm/hr), and a 6 in/hr (15.2 cm/hr) rainfall event for 20, 30 and 30 minutes respectively. Each wattle was placed on a shallow slope with a 8H:1V slope angle. According to their results, the percent soil not filtered from the 9-inch straw wattle was 65.7% and the 12-inch wattle was 80.5% during the 4 in/hr (10.2 cm/hr) event. Due to their inability filter the runoff, both straw wattles were not analyzed for the 6 in/hr (15.2 cm/hr) event (Kelsey, Johnson, & Vavra, 2010). Rills were also apparent under the 4 in/hr event showing water had flowed underneath the device and may or may not be filtered through the straw wattle. However, according to the study, these tools reduced the amount of soil loss as compared to bare soil controls, but, their study did not evaluate

straw wattles placed on slopes angles higher than 8H:1V such as those much steeper slopes found in our case study (1.5H:1V). Kelsey et. al. (2006) also focused more on sediment loss rather than slope stability, which is not generally a concern for shallow inclined slopes.

From observations made by Granite, some advantages and disadvantages of straw wattles were found (Gehling, 2010).

Some advantages include:

1. For use in sediment traps and check dams, wattles have proven to be relatively effective measures. Check dams/sediment traps constructed out of 3-inch rock in a “V” or “C” configuration and lined at the top with a piece of straw wattle seem to trap surface run-off well.
2. If constructed properly according to installation methods discussed earlier, wattles have been observed to be effective on the gentler slopes on the project, with the aid of vegetation.
3. Wattles seem to enhance growth of vegetation along the wattle line as opposed to slopes where the wattle is not present. This could be caused by a couple different possibilities: wattles may trap sediment/nutrient runoff that makes vegetation growth more optimal, and/or wattles and the area the wattle is installed in may become wetter for a longer period than a slope without wattles.

Some observed disadvantages include:

1. Water on steep slopes tends to erode the soil on the downslope side. This eventually undermines an entire section of the wattle and leads to rilling (channelizing) or general wattle ineffectiveness.
2. If the wattle is not installed in a level plane, the wattle tends to direct water to the lowest elevation of the wattle, thus focusing water in one spot instead of distributing across the slope. This leads to rilling, wattle failure, and/or possible slope saturation.
3. Wattles do not filter water, but only trap it until the liquid flows over or under device.
4. Wattles installed on bare slopes (no vegetation/hydroseed) appear to be ineffective regardless of spacing.

2.4 Straw Wattle Testing

To determine if straw wattle weights affected the factor of safety against surficial slope failure, tests were completed to find the wattles dry and saturated weight. The weight of soil accumulated by those wattles and the time needed to dry the wattles to their original state was also verified.

New and used straw wattles were taken from the project site and analyzed for saturation properties. A new wattle is defined as one in pristine condition that has not been installed and has been in its original wrapping until installation. A used wattle is defined as one that shows significant degradation due to environmental conditions and has shown some accumulation of soil material within the fabric.

A standard 10-foot straw wattle was divided into 10 one-foot sections. Each section was placed in a 5 gallon bucket and water was allowed to fill the bucket until completely full. A 1 kg weight was placed on top of the wattle to ensure that the device was completely under water for the duration of the test. Each straw wattle section was tested for one specific time amount (i.e. 15 min, 30 min, 1 hr., etc.). Time variations for the test ranged from 15 minutes to 24 hours. After each test, the wattle was immediately weighed.

The drying time for a new straw wattle was also tested. A 1-foot section was placed under water for approximately 4 hours to allow total saturation. The wattle was then placed into a 5 gallon bucket, weighed, and recorded for a period of thirteen days.

2.5 Straw Wattle Results

From the testing procedure above, it was found that a straw wattle was saturated within a small amount of time. Figure 4 shows the time-saturation relationship of the straw wattle. Granted, from this figure, only water content is plotted and not saturation. However, it was assumed that as the water content would plateau, at approximately 15 minutes, the saturation would be near 100%. Therefore, a straw wattle becomes fully saturated within 15 minutes of soaking in water. Considering a new straw wattle is wrapped in plastic, therefore not subject to precipitation, the initial water content of a straw wattle was assumed to be zero percent.

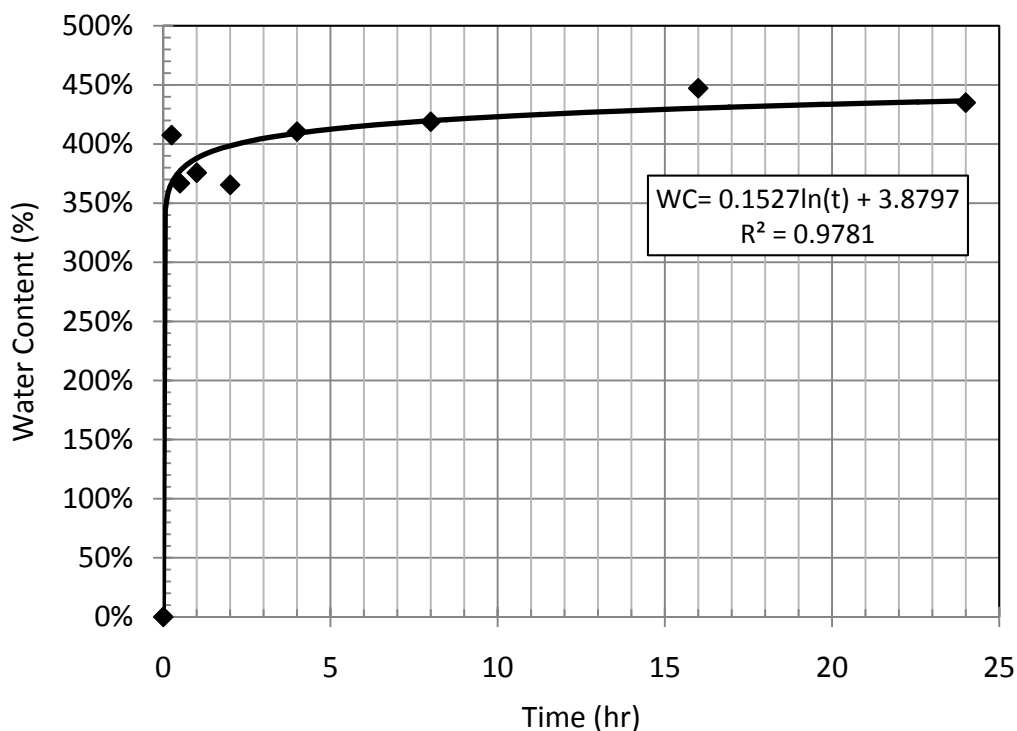


Figure 4. Straw wattle water content over time

To find a general amount of soil collected by a straw wattle in the field, the weights of new and used straw wattles were compared. The weight of a new dry straw wattle, on average, was approximately 1.1 lbs (0.00488 kN). The weight of a new saturated straw wattle was 6.0 lbs (0.0267 kN) and a saturated, old straw wattle was 7.57 lbs (0.0337 kN). It was found that the weight difference between the two was approximately 1.6 lbs (0.007kN) for a 2 meter section.

Straw wattle drying data is plotted in Figure 5. Before applying water to the straw wattle specimen, the initial mass of the device was approximately 0.530 kg. After a sufficient amount of time had passed to saturate the straw wattle, approximately 4 hours, the wattle weight was recorded as 2.840 kg, corresponding to an approximate water

content of 432 percent, which shows saturation had occurred within the ECD according to Figure 4. It seems from Figure 5 that, with increased time, the straw wattle will trend toward its initial weight, however, the conditions within a lab and the conditions in the field vary greatly.

The temperatures within the lab range from approximately 64 to 70 degrees Fahrenheit (18 to 21 degrees Celsius), whereas on site, the temperature during the wet season can range from below freezing to approximately 70 degrees Fahrenheit (0 to 18 degrees Celsius). Given this difference, one can assume that straw wattle drying most likely does not occur during the wet season. It was assumed, therefore, that straw wattles stayed saturated after initial wetting.

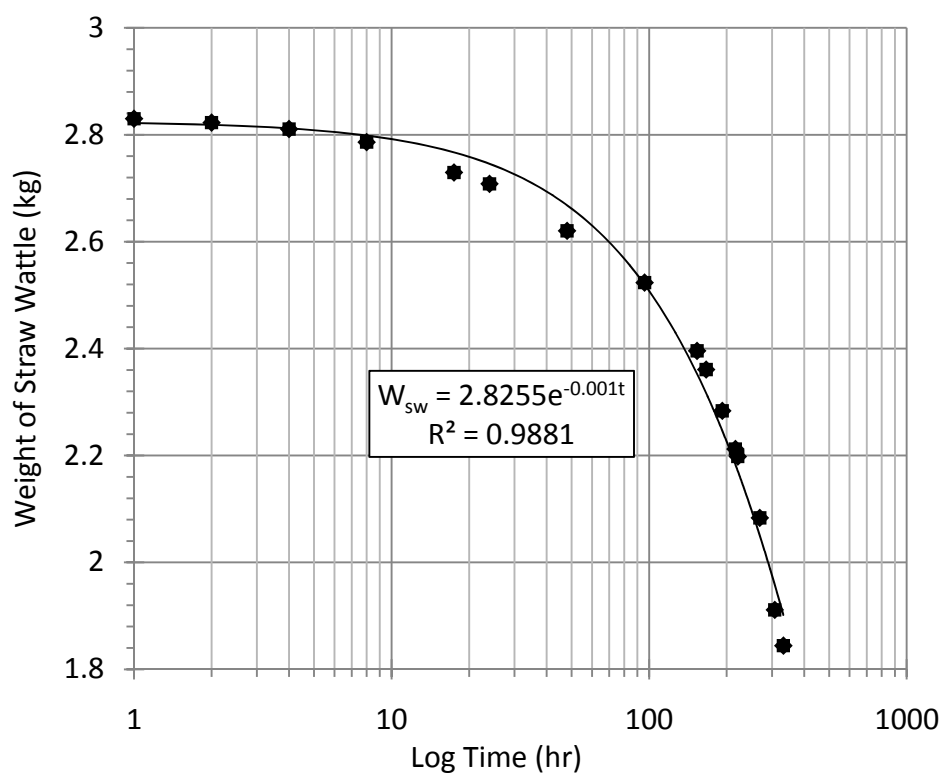


Figure 5. Drying straw wattle weight over time

Chapter 3: LiDAR Analysis

3.1 Overview

When straw wattles were installed, it was hypothesized that if a low point is created when placed water would collect and build at this point and put more weight on the soil causing a surficial slope failure. To verify that there were no low points, installment procedures were verified and LiDAR was used to find the straw wattle contours, as well as general embankment slope properties at US20PME.

3.2 Straw Wattle Installation

Straw wattles were installed according to specifications given by Granite Construction (Granite). Figure 6 shows an example of the straw wattles on-site. Originally, straw wattles, at lengths of 10 feet (3 m), were spaced at 25 feet (7.6 m) from the top to bottom of the slope and no vegetation was placed. With the increasing amount of wattle-bracketed surficial slope failures observed, the spacing was changed to 75 feet and grass seed was installed into the embankment slopes.



Figure 6. Example of straw wattle placement on-site

According to Granite, the wattles were placed level with slope contours and the spacing between, as discussed previously, was 75 feet (23 m). A sight level and string line were used to paint the wattle line. A 6-inch-wide trench was then dug using shovels along the contour line approximately 3 to 5 inches deep to avoid gouging into the slope too much (Gehling, 2010). At the connection of straw wattles, one foot of the connecting wattle was overlapped onto the new wattle. Once the wattle was set, a stake was inserted every 5 feet (1.5 m) of wattle.

3.3 LiDAR Overview

LiDAR systems have grown to be an immense tool in mapping activities for geotechnical engineering (e.g. Kayen et al. 2010). This tool has been used in many different projects analyzing cliff erosion, landslide movement, etc. throughout the world. LiDAR devices can be attached to airplanes or motor vehicles for terrain mapping or can be held stationary. For the purposes of this study, a static, stationary LiDAR scanner was used. The data from the scanner was georeferenced using a GPS unit mounted on top of the scanner using the methodology by Olsen et al. (2011). The LiDAR scanner gathers 3D information about the space around it by pulsing laser units in many different angles, which are then reflected back by the contacted surface and the range and position of the surface are recorded in reference to the scanner's position. Further, digital photographs are taken for color superposition onto the data. The scanner also records a measure of return signal strength and intensity, which provides insight regarding the material from which the pulse was reflected.

3.4 Purpose

LiDAR was used on this project for the following purposes:

- Determine fill slope inclination angles
- Determine embankment slope heights
- Observe straw wattle contour elevations and spacings
- Record failure depths to verify if surficial in nature

3.5 Observations

Fills 6, 8, and 10 were scanned with a LiDAR device. All fills showed a general slope angle of 1.5H:1V. Their height varied from 30 to 40 meters. Straw wattles spacings were determined to be 25 ft and each wattle was installed at a consistent contour around the embankment slope. These elevations and spacings can be seen in Figures 7 and 8.

The LiDAR scans documented deformations in each of the fills. These failures were, in general, a depth of 2 to 3 feet (0.60 to 0.91 m). Some failures observed were bracketed by straw wattles. There were, however, a number of failures that started and ended where no straw wattles were placed such as Figure 9.

3.6 Conclusion

With the contour observations from the LiDAR scanning and review of the installment procedures, it was verified that the straw wattles were placed at general elevation contours and no low points were observed. Because of this, it was assumed water mounding was not likely, and thus, the water mounding hypothesis was now proven incorrect.

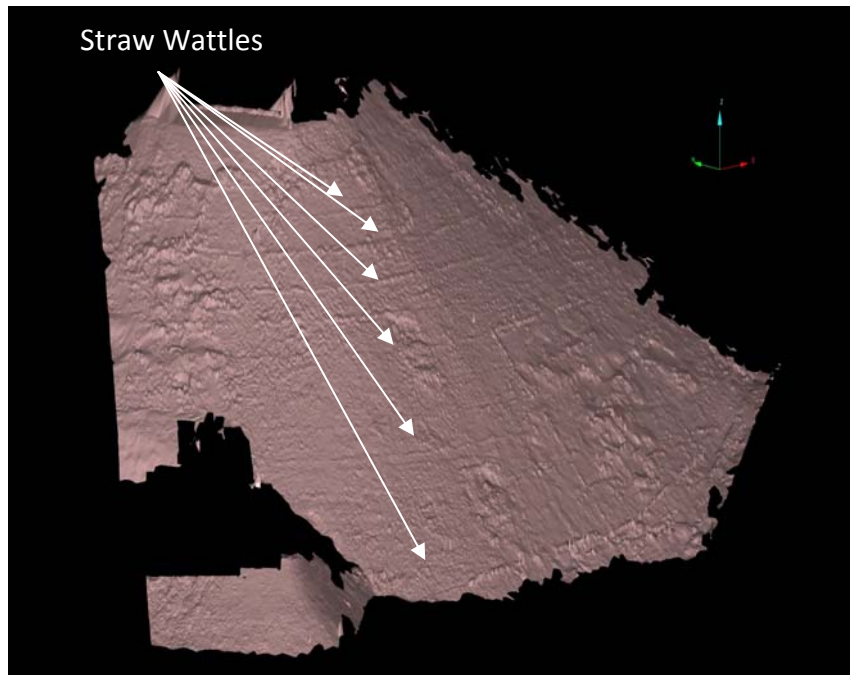


Figure 7. DTM of LiDAR scan of straw wattle elevations on slope

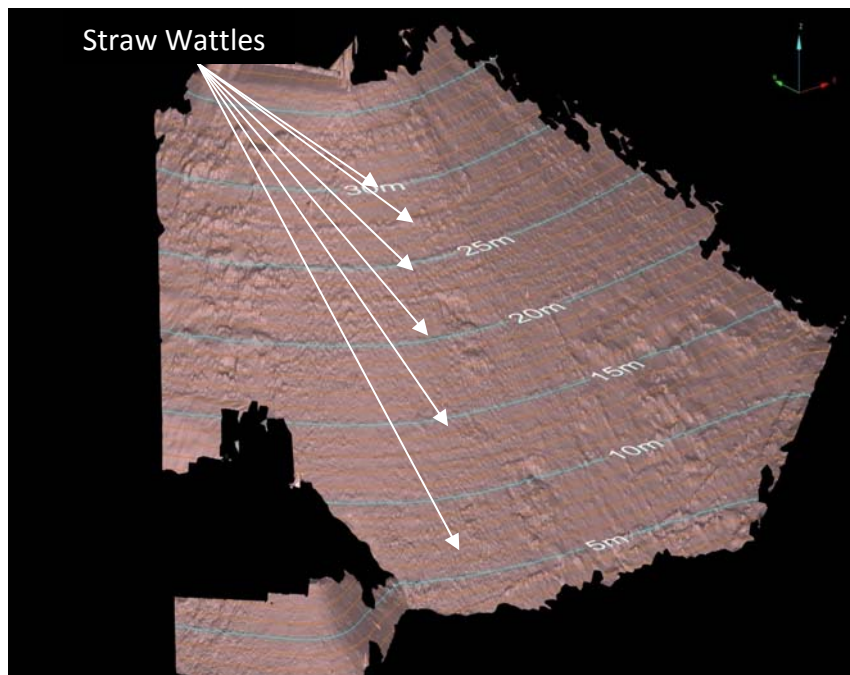


Figure 8. DTM of LiDAR scan of fill slope with constant straw wattle elevation

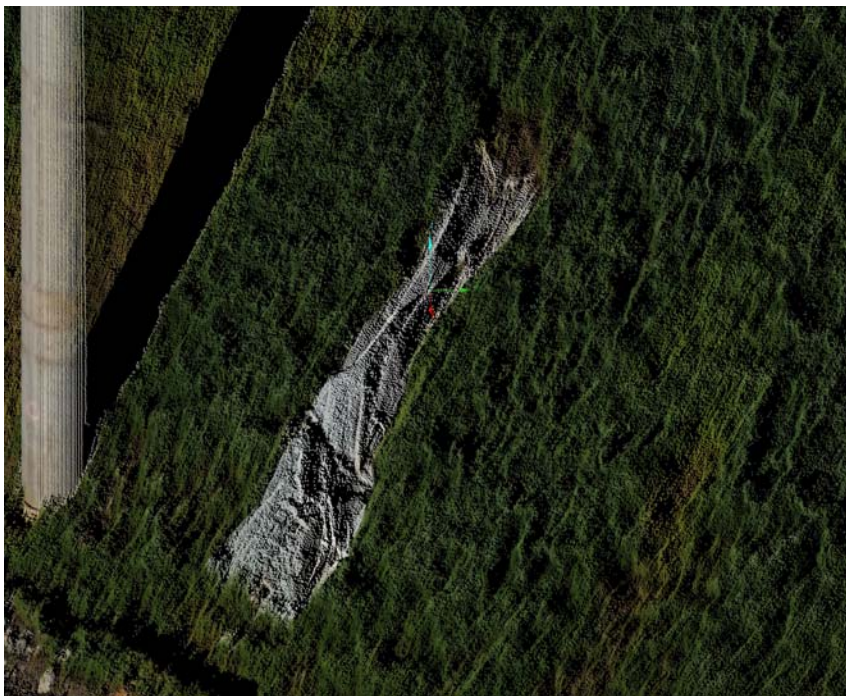


Figure 9. LiDAR survey of slope failure on US20PME

Chapter 4: Soil Testing

4.1 Overview

Once the straw wattle weights are found (or driving forces), the resisting forces must be determined. The soil's strength is this resisting force. To evaluate strength properties as well as others (e.g. hydraulic conductivity, unit weight), various tests need to be completed. These tests include:

1. Grain size distribution and hydrometer
2. Atterberg limits
3. Standard and modified compaction tests
4. Shear strength testing
5. Hydraulic conductivity
6. Swell testing

Each are discussed in the following sections and calculations completed for each test are included in Appendix B.

4.2 Testing Overview

From on-site observation, the fill soils are composed of a matrix of sand, silt, clay and gravel with some organics. Organics, in this case, are grass roots with a general depth of 6 in. (15.2 cm). According to soil boring logs provided by Granite, the construction site shows approximately 0 to 6 inches (0 to 15 cm) of topsoil underlain by approximately 12 to 30 feet (3.7 to 9.1 m) of a silt-sand mixture. Below this soil are alternating layers of silt and sandstone (Foundation Engineering, et. al. 2004).

Soil samples were collected from Fills 6, 8, and 10. These soils were sampled in the spring of 2010 from areas of observed slope failures. Because of inclement rainfall

between time of failure and when soil was gathered, the samples for testing were allowed to air dry prior to testing.

4.2.1 Grain Size Distribution Analysis

The grain distribution of soil particles can influence engineering properties such as strength and hydraulic conductivity, which will ultimately govern the soil behavior and performance. This distribution analysis is also used to classify the soil, which is important to determine if it is suitable for use in roads, dams, or embankments. The distribution can also influence the maximum dry density and optimum water content of the soil, which will be discussed in section 4.2.3.

In a sieve analysis, a series of sieves are stacked from coarse to fine meshes (top to bottom) to allow soil separation by size. A pan is used at the base to catch all grain sizes smaller than 0.003 in (0.075 mm) in diameter. Soils are sifted through several sieves (Table 1) in accordance with the American Society for Testing and Materials (ASTM) D421 and D422 procedures. The stacks are shaken for 10 minutes in a mechanical sieve shaker and the amount retained on each sieve following shaking is weighed.

Table 1. Typical sieve openings

Sieve Number	Sieve Opening	
	(in)	(mm)
4	0.187	4.750
10	0.079	2.000
40	0.017	0.425
100	0.006	0.150
200	0.003	0.075
Pan	-	-

If the percentage by weight retained in the pan is greater than 50 %, a hydrometer analysis is performed on that sample. A hydrometer test uses Stoke's Law for falling spheres in a fluid. This law states that, in general, the terminal velocity of fall depends on the diameter and the density of the object falling and the liquid density it is falling through. For the hydrometer test, the soil's grain size can be established recording the falling time and the new density of liquid thereafter. The density of the suspended soil can then be found by examining the percentage of particles of a grain size diameter still suspended in the liquid. This calculation, however, is highly dependent on the mass of soil used.

In accordance with ASTM D421 and D422, 50 grams of oven dried soil with particle diameter smaller than 75 μm (#200 sieve) is used in a hydrometer test. The soil is mixed with a 4% solution of sodium hexametaphosphate and left for 16 hours for deflocculation. This process allows the soil particles to fall without attaching themselves to each other. The soil mixture is then mixed for one minute, placed in a sedimentation cylinder, shaken 60 times per minute and then measured with a 152H hydrometer in log time increments.

4.2.2 Atterberg Limits

While grain size distribution curves provide insight on the engineering properties of soil, fine-grained soils can exhibit different behaviors depending on their water contents. Dr. Albert Atterberg identified six different limits of soil behavior based on increasing water content: upper limit of viscous flow, liquid limit, sticky limit, cohesion limit, plastic limit, and shrinkage limit. For this study, we will concentrate on the plastic,

cohesion, and liquid limits shown in Figure 10. A more detailed discussion can be found in (Holtz, Kovacs, & Sheahan, 2010).

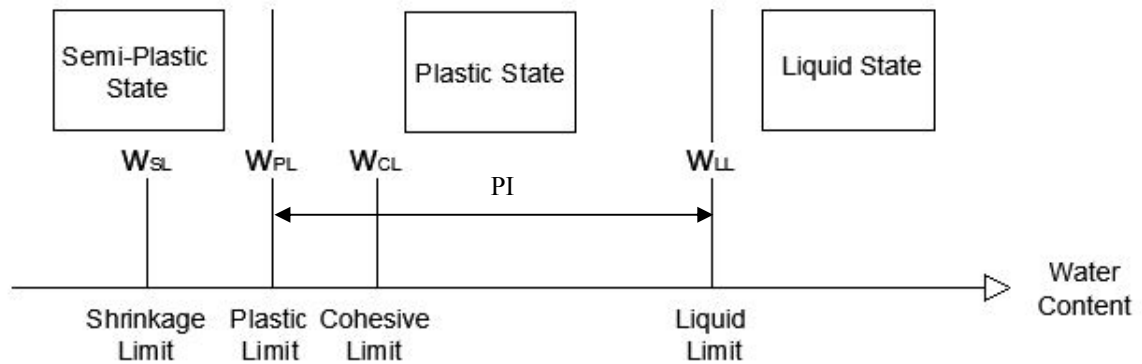


Figure 10. Atterberg Limits and soil states (Modified from Ecoles Des Ponts, 2010)

The liquid limit (LL) is the lowest moisture content corresponding to viscous flow in the soil or the highest point of the plastic state of a soil. The plastic limit (PL) is the lowest moisture content of the plastic state of a soil and the plasticity index (PI) is the moisture content range in between (Figure 10) (Holtz, Kovacs, & Sheahan, 2010). Visually, the plastic limit is the water content at which the soil begins to exhibit a plastic behavior with increasing water content. The liquidity index (LI) provides a ratio for determining how close the soil is to a liquid state. At the plastic limit, the LI is zero and at the liquid limit the liquidity index is equal to 1.

$$LI = \frac{(WC - PL)}{LL - PL} \quad (\text{Eq. 3})$$

where WC is the natural water content of the soil. When the liquidity index is zero, the soil also has a brittle fracture when sheared. Alternatively, when the liquidity index is 1

or above, the soil will behave as a very viscous liquid when sheared (Holtz, Kovacs, & Sheahan, 2010). Between the two points, a cohesion limit is achieved when the grains cease to cohere to each other, which can result in a significant strength loss in the soil (Holtz, Kovacs, & Sheahan, 2010). Atterberg, to find these important soil limit states, created a standard test known as the Atterberg limits test.

Three Atterberg limits tests were performed on each fill material according to ASTM D4318. To determine the liquid limit, a Casagrande tool was used (Figure 11, left). Three threadings were molded to assess the plastic limit for all bulk samples.

The Casagrande device is first calibrated using a Casagrande “grooving” tool to standardize the bowl’s drop height at 0.39 inch (1 cm). The soil specimen is then spread across the dish and a ditch line is dug, using the same Casagrande “grooving” tool. This is dug into the center to create an indentation approximately 0.0787 in (2 mm) in width. Great care is taken to eliminate air pockets within the soil and between the soil and dish surface when placed into the device. The dish is then dropped 15 to 35 times until an approximate 0.511 in (13mm) of soil in length closes the groove. This is repeated at least three times to formulate an accurate blow versus moisture content curve. The moisture content at which 25 blows is reached is deemed the liquid limit.

To determine the PL, a soil specimen is rolled on a Plexiglas surface, shown in Figure 11, to a diameter of 0.12 inches (3 mm) where the soil essentially crumbles. This is repeated at least three times and the moisture contents of each roll are taken. An average moisture content is recorded and the result is the plastic limit.

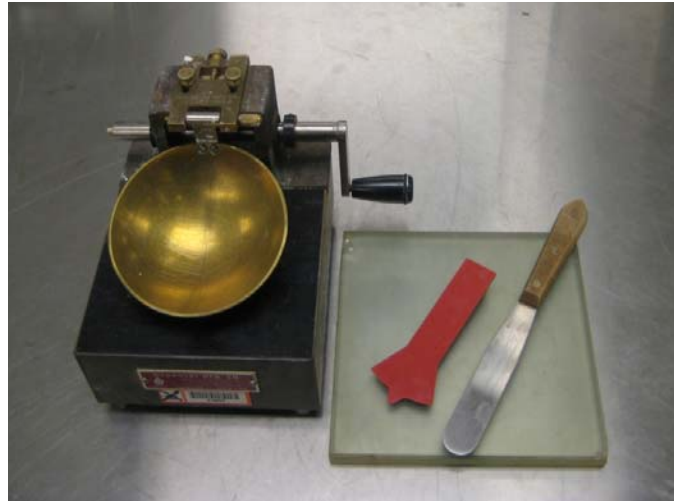


Figure 11. Casagrande device, grooving tool, and plastic limit equipment

4.2.3 Standard and Modified Compaction Test

Soil compaction is commonly used to improve a soil's strength by removing voids and densifying the soil. When soil is properly compacted, the following benefits can be achieved:

- Increase in shear strength. By increasing the density, the normal stress on the soil is increased. Also, there is more grain-to grain-contact which can provide more shear resistance.
- Decrease in Permeability. Decreasing the voids of a soil deposit decreases the area through which water can flow. This is very important for clay liners.
- Decrease in shrinkage potential.
- Decrease in compressibility. This can lead to decreased settlements at a site, which reduces building damage.

The degree of compaction possible depends on the type of soil, the method of compaction, the energy provided by the method, and the water content. For our case

study, modified and standard proctor may not correlate well with the actual force applied to soil compaction. As we will see in the compaction test results and comparisons section, 109% of the standard maximum dry density was achieved which shows that the standard compaction test does not adequately show the in-field forces applied to the soil for compaction. However, to understand this, some explanation is needed about standard and modified compaction tests and how they are completed.

The tests most commonly used to calculate the theoretical maximum density of a soil are the standard and modified compaction or proctor tests. These tests can be completed in three different methods (A, B, and C as described in ASTM D698 and D1557). These are also seen in Table 2 and Table 3. Each method chosen is dependent on the grain size distribution of that material. In Figure 12, a standard compaction and modified compaction test procedure was created following both ASTM standards discussed above.

In the compaction test, an optimum moisture content and maximum dry density of the soil are determined from a plot relating density and moisture content. The apex of the curve is then chosen as that maximum dry density and optimum moisture content of the tested soil.

Table 2. Compaction methods for standard compaction tests

Standard Compaction Test			
	Method A	Method B	Method C
Hammer Wt.	5.50-lbf (24.5-N)	5.50-lbf (24.5-N)	5.50-lbf (24.5-N)
Mold Diameter	4 in (101.6-mm)	4 in (101.6-mm)	6 in (152.4-mm)
Material Passing	No. 4 (4.75-mm) sieve	3/8-in. (9.5-mm) sieve	3/4-in.(19.0-mm) sieve
Layers	3	3	3
Blows per Layer	25	25	56

Table 3. Compaction methods for modified compaction tests

Modified Compaction Test			
	Method A	Method B	Method C
Hammer Wt.	10.00-lbf. (44.48-N)	10.00-lbf. (44.48-N)	10.00-lbf. (44.48-N)
Mold Diameter	4 in (101.6-mm)	4 in (101.6-mm)	6 in (152.4-mm)
Material Passing	No. 4 (4.75-mm) sieve	3/8-in. (9.5-mm) sieve	3/4-in.(19.0-mm) sieve
Layers	5	5	5
Blows per Layer	25	25	56

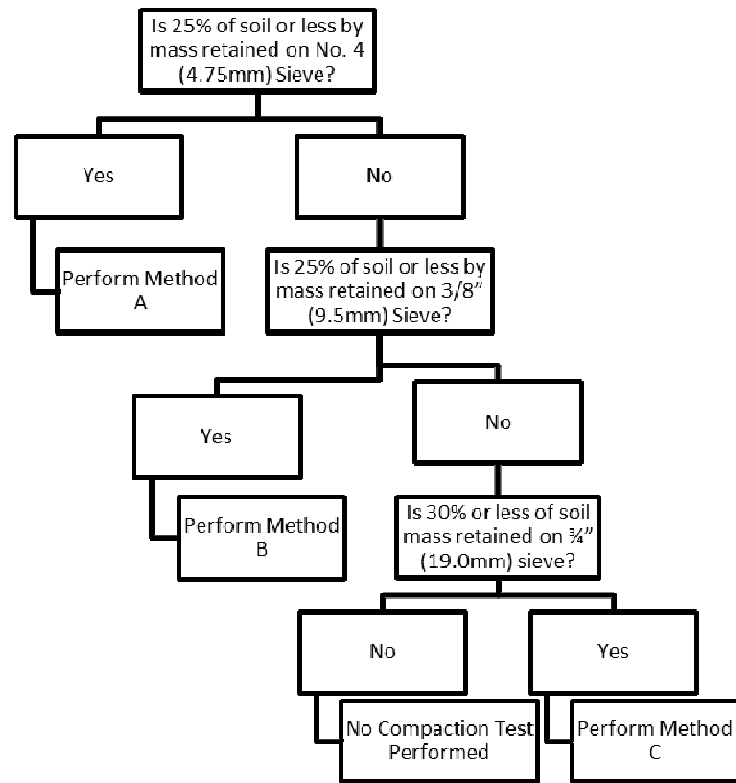


Figure 12. General compaction test procedure

An example of standard compaction test results is seen in Figure 13. Notice that the data plotted is compared with a line of optimums and zero air voids curve. The line of optimums is a curve fitting all optimum moisture contents and maximum dry densities of a soil using different compactive effort. The zero air voids curve is a theoretical curve where the soil is 100% saturated leaving no air pockets or voids within the compacted specimen. Although possible, this line is not physically achievable through compaction alone.

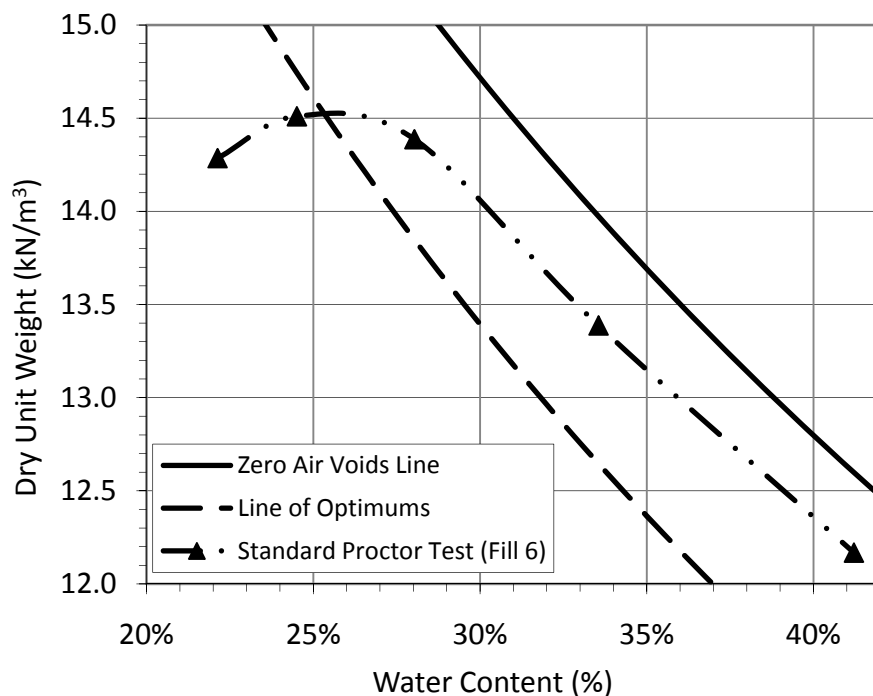


Figure 13. Example of standard compaction test results

A total of three standard compaction tests were completed on each soil gathered. The standard proctor test was used to be consistent with field compaction tests. One modified proctor test was also completed on soil gathered from Fill 6 to compare its maximum dry density and optimum moisture content to the standard.

4.2.4 Shear Strength Testing

Strength properties can be found using laboratory tests such as the direct shear and triaxial test. The direct shear test subjects a soil sample to increasing lateral load, ultimately developing a shear failure plane of zero degrees. This test, although inexpensive and fast, tends to form high stresses at the edges of the specimen, causing non-uniform stresses within the soil and most likely skewing test results. For this reason, the triaxial test is a more reliable test and was used for this study.

Triaxial tests can compress or extend a soil to find the soil's compressive or tensile strength. In this study, since straw wattles are applying a downward force onto the fill slope, triaxial compression tests were administered.

Triaxial compression of a specimen can be completed by three different tests. These are unconsolidated undrained (UU), consolidated undrained (CU), and consolidated drained (CD) triaxial compression tests.

In selecting one of the three tests, field pore water pressure (PWP) conditions need to be known or estimated based on experience. CD triaxial compression tests are used to simulate field conditions where soils fully drain as loads are applied. For example, a drained test would be performed if loads are applied on soils so slowly that all the excess PWPs decrease to zero within the soil. The types of soils used for such a test are coarse sand and gravel specimens. Fine sands and silts can also be CD tested, if the PWPs dissipate to zero. These tests are also used for long term loading on cut slope projects, embankments, earth dams with steady seepage and foundations on clay soils.

The CU test does not allow excess PWPs to dissipate. For these types of tests, reasonable results can be found for field conditions involving soil deposits being loaded over a period of several days or weeks. This test is used for projects involving building foundations, earth embankments, highway foundations, or earth dams during rapid drawdown.

For soils in a quickly constructed earth dam, underneath a rapidly loaded foundation, or for fine-grained soil cut material, strength parameters are calculated using UU tests.

Each test's purpose, although used for different construction practices, is to find the appropriate strength parameters (friction angle (ϕ') and cohesion (c')). These tests best describe what forces are applied to soil in the field and how the soil's strength reacts to those forces.

Various assumptions are made about the soil and its PWP conditions at failure. If one assumes that no drainage takes place in the soil, a total stress approach is taken where total and undrained shear strength is calculated from the triaxial test. This, however, may be too conservative and an effective stress approach is needed to be more accurate.

In this procedure, one must estimate the hydrostatic PWP and the initial and applied field stresses if more in depth in-situ testing is not available. Since these pressures can be controlled in lab tests (triaxial and direct shear testing), this approach is much more satisfying than the total stress approach.

The CU triaxial test, as detailed in ASTM D4767, compresses an undrained soil sample that has been saturated and consolidated to a stress where the soil's strength cannot compensate for the load applied on it. Once the sample has reached this limit, it fails and shears. This test measures PWPs within the specimen and allows for calculation of the soil's friction angle (ϕ') and cohesion (c'). The CD test also allows calculation of friction angle and cohesive strength, however, PWPs are not calculated since it is in a drained condition where there is no apparent water. Finally, the UU test (ASTM D2850-03a) compresses a sample to failure similar to the previous tests, however, a soil's friction angle cannot be determined. A soil's ultimate shear failure strength, however, can be calculated. This strength equals the soil's initial cohesion (c') earlier discussed.

For the purposes of this thesis, it was assumed that the fill was fully consolidated and PWP's were apparent when the slope failures occurred. Therefore, a consolidated undrained (CU) triaxial compression test was administered to determine the strength parameters of the fill material. Figure 14 shows an example of a triaxial apparatus and loading frame used for this test. The CU test was organized into four phases: preparation, saturation, consolidation, and shearing.



Figure 14. Triaxial and cell apparatus

4.2.4.1 Preparation

Following ASTM D694, a soil specimen was constructed using a standard compaction test at a moisture content of 23 percent, matching soil densities in the field. The dry unit weight of each specimen was approximately 93 pcf (14.6 kN/m^3) with a

corresponding moist unit weight of 114 pcf (17.9 kN/m³). The specimen was then trimmed to the shape of a cylinder with approximate diameter of 2.8 inches (71 mm) and height of 4.2 inches (107 mm). The trimmings were placed into pre-weighed containers and placed in a heating oven overnight to find the exact initial moisture content of the specimen.

The triaxial apparatus was then assembled. Six membranes with diameter of 2.8 inches were cut, greased, and placed on the top and bottom platens. Earlier, the bottom platen was secured to the apparatus' bottom plate, and this connection was tested for leaks. Shear keys were then placed into each top and bottom platen to prevent the soil from moving laterally during axial shear. Filter disks were placed in the sides of both platens to allow water/air to filter out of the specimen into the rest of the cell.

The soil was then centered on the bottom platen. Overall, small cuts needed to be made to ensure full seating on this platen with the shear key placed. Filtering geotextile was then cut and wrapped around the specimen, making sure all filter slots were snug around the soil, and taped together where both edges met. This filter was used to encourage horizontal seepage into the specimen.

A, vacuumized, stretched, 10-in. tall, 2.8-in. diameter, and 0.012-in. thick membrane was then placed around the specimen, paper, and bottom platen. The top platen was placed on top of the soil specimen. The filter geotextile was placed to cover the filter disks within the top and bottom platens, to again, encourage full saturation of the specimen. The vacuum on the stretched membrane was then released with the top drain connected to the top platen. The cell wall of the apparatus was then installed and

the top plate was tied to the tie rods. The piston was then screwed into the top platen till secure and the top and bottom drain to the specimen were tied together with a T-valve.

4.2.4.2 Saturation

Following preparation, the triaxial apparatus is then filled with de-aired water and all air is displaced from inside the cell. The specimen, at this time, is not filled with water because the membrane wall released around it blocks water from entering. The pressure valve, on the top plate of the triaxial apparatus is first open to the air, to allow for all pressure to dissipate from the inside of the apparatus, and then turned to the pressure regulator. The pressure transducer, also on the top plate of the apparatus, is turned to air, again to dissipate all pressure inside the cell, and turned to the transducer to record the cell pressure applied on the soil as well as the pore pressures within the apparatus.

Following water application to the triaxial apparatus, the bottom drain, attached to the bottom platen underneath the soil specimen, is attached to a CO₂ tank while the top drain, attached to the top platen, is led out to the outside air. Since CO₂ is heavier than air, the CO₂, in theory, should displace all air within the soil sample. To do this, the gas mixture is flushed through the soil for 20 minutes.

Following CO₂ flushing, de-aired water is flooded through the soil using the bottom drain making sure no air is present within the drain or the connecting apparatus between the de-aired water and bottom drain. Approximately 2 liters of water is streamed through.

Next, to eliminate space between the membrane, the soil and the two platens, water is inserted into the triaxial apparatus for approximately 25 minutes and then closed

off. During the 25 minutes, a linear variable displacement transducer (LVDT) measuring device is attached to the piston, which is, from before, attached to the top platen within the apparatus. The LVDT monitor is a device to measure displacement using voltage. The load cell, pressure transducer, volume change device (VCD), and the LVDT, which all measure values in volts, were calibrated prior to testing. The top drainage line is then closed with a cap and both outlets on the top plate are opened to the air. The “zero voltage reading” is taken for the cell pressure transducer and the LVDT.

4.2.4.3 Consolidation

In order to find the correct rate of load application for the specimen, the sample is consolidated. First, the top and bottom drain lines, at the bottom of the triaxial apparatus, are attached to the VCD, eliminating all air bubbles between the two lines before connection. The initial VCD reading is recorded. The sample is then consolidated with 25kPa cell pressure applied and de-aired water is allowed to flush through. This consolidation is run for approximately one hour.

After one hour, the VCD is again read and the pressure transducer is switched over to record back pressure. The reading here is the initial back pressure and 100kPa back pressure is calculated using this value with calibration data found earlier.

The pressure transducer is then switched to read cell pressure, the central valve is closed, and 125kPa pressure is applied. The drain valve is closed and the central valve is opened. The back pressure is then brought up to 100kPa. The pressure transducer is switched back to cell pressure and the voltage reading is recorded. Then, the drain valve is opened for 15 minutes and the cell pressure is again read after.

A B-value is now found for the specimen. The B-value in a triaxial test is the difference in pore pressure divided by the difference in cell pressure also known as the total minor principal stress. This value measures the percent saturation of the specimen and a satisfactory saturation percentage used was 97%.

To find this value, the initial cell pressure and pore pressure are recorded. The cell pressure is then increased by 100kPa and the pore and cell pressures are recorded after 10 minutes. The difference is calculated and a B-value is found.

For many of the tests completed, the initial B-value was below 97%. For most cases, the back pressure was increased by 25 to 50kPa until a satisfactory B-value was recorded. For a few cases, the sample was left overnight and a satisfactory B-value was recorded the following day.

Following a B-value check, a target cell pressure was applied to the soil specimen. Example cell pressures applied are 394kPa, 197kPa, and 186kPa with back pressures of 250kPa, 125kPa, and 150kPa, respectively. Noticeably, these are fairly high pressures. The reason for using these was because we wanted to find out what effect straw wattles had on the overall stability of the slope. With these high pressures, we could gain the slope's overall friction angle and cohesive strength and analyze those values with straw wattle placement. Once the cell pressure is applied, the central valve is opened after 30 minutes and the specimen is consolidated for 12 hours.

4.2.4.4 Shearing

After 12 hours, the consolidation curve is analyzed to find the t_{50} value. To get the t_{50} value, the t_{100} value must first be found. This value, as shown in Figure 15, is

described as the time where 100% primary consolidation has occurred in the soil (Holtz, Kovacs, & Sheahan, 2010). Theoretically, this value is the intersection of the primary consolidation curve and the secondary consolidation curve. For this study, the t_{100} value was found using trendlines for both curves and finding the intersection point of the two. Once this value was found, and using the initial t_0 value, we can find the t_{50} value.

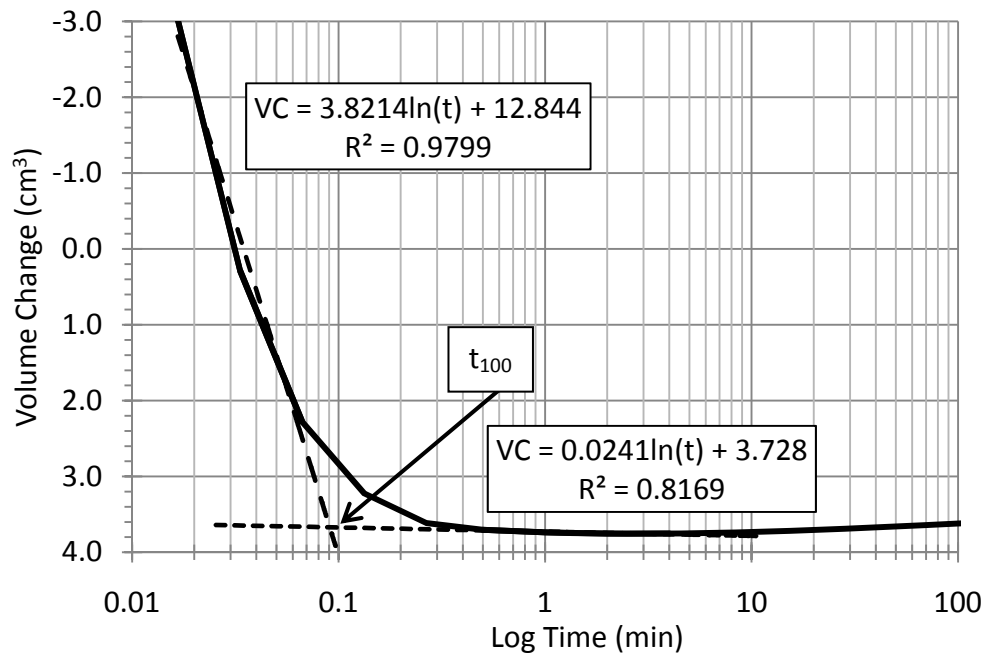


Figure 15. 144kPa consolidation curve

The t_{50} value is defined as

$$t_{50} = \frac{(d_0 + d_{100})}{2} \quad (\text{Eq. 4})$$

where d_0 is the initial displacement or volume change and d_{100} is the volume change at 100 percent consolidation. Both values are found using corresponding t_0 and t_{100} values from the consolidation curve. With the t_{50} value, a strain rate can be analyzed

to ensure that pore pressures are equalized throughout the test. According to ASTM D4767 the strain rate (ϵ') for cohesive soils is defined as

$$\epsilon' = \frac{4\%}{(10 * t_{50})} \quad (\text{Eq. 5})$$

However, when finding the strain rate, it was determined that these were far too fast for the loading and triaxial cell apparatus. Using this knowledge, the percent strain till failure was reduced to 0.05% for each test. Example strain rates include 0.167 mm/min, 0.214 mm/min, and 0.210 mm/min for cell pressures of 36kPa, 72kPa and 144kPa.

These rates were then entered into the loading frame apparatus, and a ball bearing was set atop the piston, which was then centered below the load cell. The central valve was closed to guarantee no drainage and the pressure transducer was set to read pore pressure. The soil was then sheared. Figure 16 shows the soil in the apparatus after shearing has completed and sliding has occurred within the soil.

The results of this test relate stress, effective and total, with the shear strength of the soil. A graph is then created relating the two components and several Mohr's circles are developed (Figure 2). The Mohr's circles represent the stresses of a soil at failure and help to determine the shear strength of a soil at failure at each stress. These circles are created from each consolidated undrained triaxial compression test and help to define a Mohr-Coulomb failure envelope, previously mentioned.

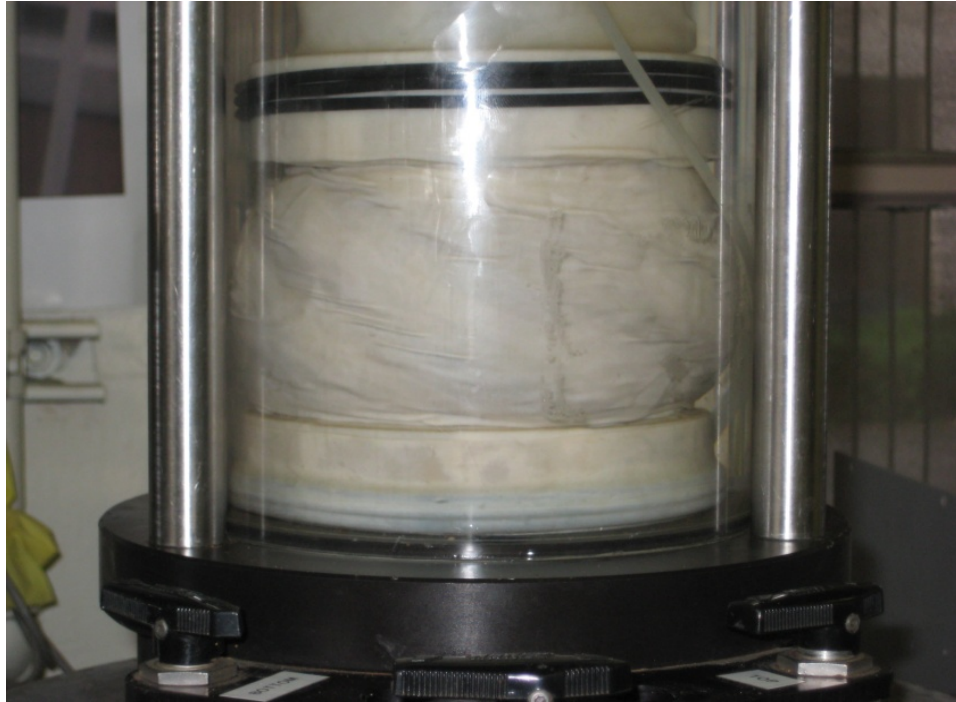


Figure 16. Failed soil in consolidated undrained triaxial test

The Mohr-Coulomb failure envelope (Figure 2) yields a simplified relationship between the stress and shear strength of a soil at failure using a best fit line tangent to each Mohr circle developed. A soil at failure is defined here as the largest ratio of the stress applied by the load cell (σ_1) to the stress applied by the surrounding water (σ_3). In other words, the ratio of these two stresses is greatest when the soil fails. This Mohr-Coulomb failure envelope also gives a limit at which failures can occur within a soil. For example, a Mohr's circle below the line represents a stable condition where no failure will occur within the soil. Above the line, no shear strength failure can occur with a corresponding principle stress. The Mohr-Coulomb failure envelope is simplified to be linear, however, as discussed earlier, in reality; this criterion is represented with a curve.

Three tests were performed on the soil samples from Fill 6. Figure 17 shows an example of the end profile of the tested soil. One can see from this figure that the soil has failed along the line drawn which represents the shear failure plane.

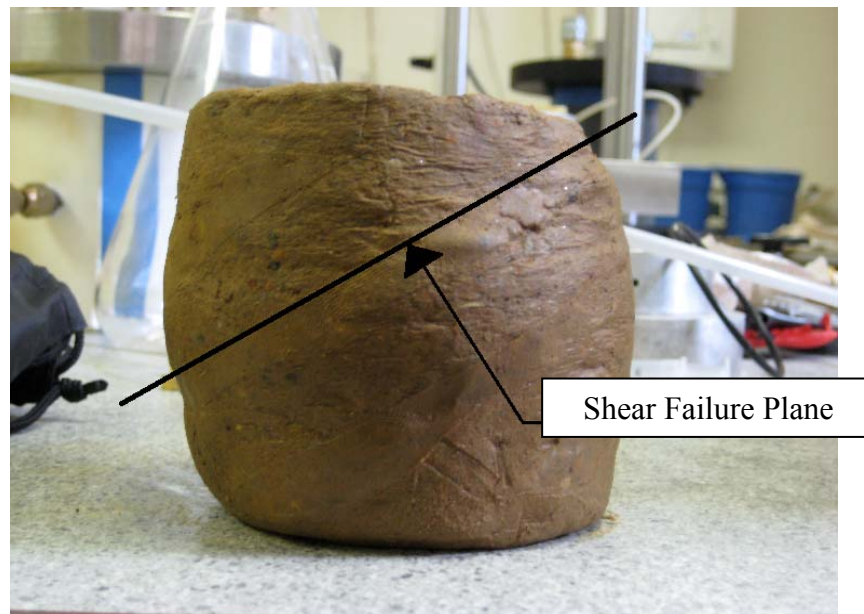


Figure 17. A soil sample at failure after a CU triaxial compression test

4.2.5 Hydraulic Conductivity Testing

The hydraulic conductivity is the rate at which water flows through a soil material. This property can be very high for cohesionless sands and gravels or very low for silts and clays. Using this soil identity, one can find how fast a soil drains when a load is applied and helps to determine if the soil acts in a drained or undrained manner. This, in turn, can also determine if an effective or total stress analysis is needed when beginning a triaxial test.

The vertical hydraulic conductivity was determined through one-dimensional consolidation tests in accordance with ASTM D2435. It should be noted that prior to

completing this test, due to the prior compaction of the placed soil, the hydraulic conductivity tested in the lab can be somewhat different than that in the field. In this test, a disc of soil measuring approximately 1-inch (25 mm) in height was placed in a metal ring of an approximate inner diameter of 2.4 in (62 mm). The soil-ring assembly was then placed between two filter discs and centered below a point load. The assembly was then subjected to weights ranging from 0 to 16.7 tons (0 to 1600 kPa). The deformations were recorded when each weight was placed over a certain period of time. For the most accurate results, an undisturbed soil sample is used. However, to model field conditions, the material was compacted in a standard proctor mold, and extruded into the metal ring.

4.2.6 Swell Testing

Some clay soils can expand and/or contract due to fluctuations in the soil's water content. The swelling of clays can induce considerable distresses and thus serious damage to civil engineering structures (Al-Homoud, et. al, 1995). These damages can happen over many wetting and drying cycles and can possibly cause desiccation cracking on a fill slope over time. This can then lead to increased rainfall seepage, increasing PWP's, and decrease the factor of safety against surficial slope failure.

4.2.6.1 1D Swell Test

To determine if the soil was indeed expansive, a one-dimensional swell test, according to ASTM 4546-08, was conducted similar to the one-dimensional consolidation test described previously. The soil was compacted according to ASTM D698 at approximately optimum moisture content. The soil was then placed into a brass ring with an inner diameter specified above. The soil-ring assembly was then placed

between two filter discs and again centered below a point load. Generally, several loads are applied to the soil. However, since failures occurred at the top of the fill where approximately no load is applied to the soil, the seating load was only used for our testing. Readings were taken before, during and after sufficient time had occurred for full expansion of the soil.

4.2.6.2 Free Swell Test

Following a one-dimensional swell test, a free swell test was performed according to the procedure outlined by Holtz, Kovacs, & Sheahan (2010). Approximately 10 cm³ of on-site soil was placed in a 100 ml graduated cylinder and was filled to 100 ml with de-aired water. To encourage full saturation of the soil, a glass wand was used to mix the soil and water together. An initial height was recorded and another was the following day.

4.3 Testing Program Results

4.3.1 Soil Classification and Atterberg Limits

The soil in the failed slope areas, on average, was a silty sand with some clay and trace gravel (SM). Table 4 shows this average including a summary of the Atterberg limits, gradations, and Unified Soil Classifications (USC) for each fill. A plasticity chart is also provided in Figure 18. The average gradation included 18% gravel, 33% sand, 30% silt, and 19% clay. The gradations are included in Figure 19. Although each gradation varied slightly between Fills 6, 8 and 10, overall, they were relatively similar and differences are most likely due to the natural variability in the fill.

Table 4. Test result summary and soil classification

Fill 6		Fill 8		Fill 10		AVERAGE	
Soil Type	%	Soil Type	%	Soil Type	%	Soil Type	%
Gravel	7.9	Gravel	32.3	Gravel	13.5	Gravel	18
Sand	30.3	Sand	40.9	Sand	27.5	Sand	33
Silt	39.9	Silt	15.9	Silt	35.6	Silt	30
Clay	21.8	Clay	10.9	Clay	23.4	Clay	19
Atterberg Limits	%WC	Atterberg Limits	%WC	Atterberg Limits	%WC	Atterberg Limits	%WC
Liquid Limit	54.3	Liquid Limit	44.6	Liquid Limit	46.7	Liquid Limit	48.5
Plastic Limit	39.2	Plastic Limit	27.8	Plastic Limit	31.8	Plastic Limit	32.9
Plasticity Index	15.1	Plasticity Index	16.8	Plasticity Index	15.0	Plasticity Index	15.6
USCS Soil Type	MH	USCS Soil Type	SM	USCS Soil Type	ML	USCS Soil Type	SM

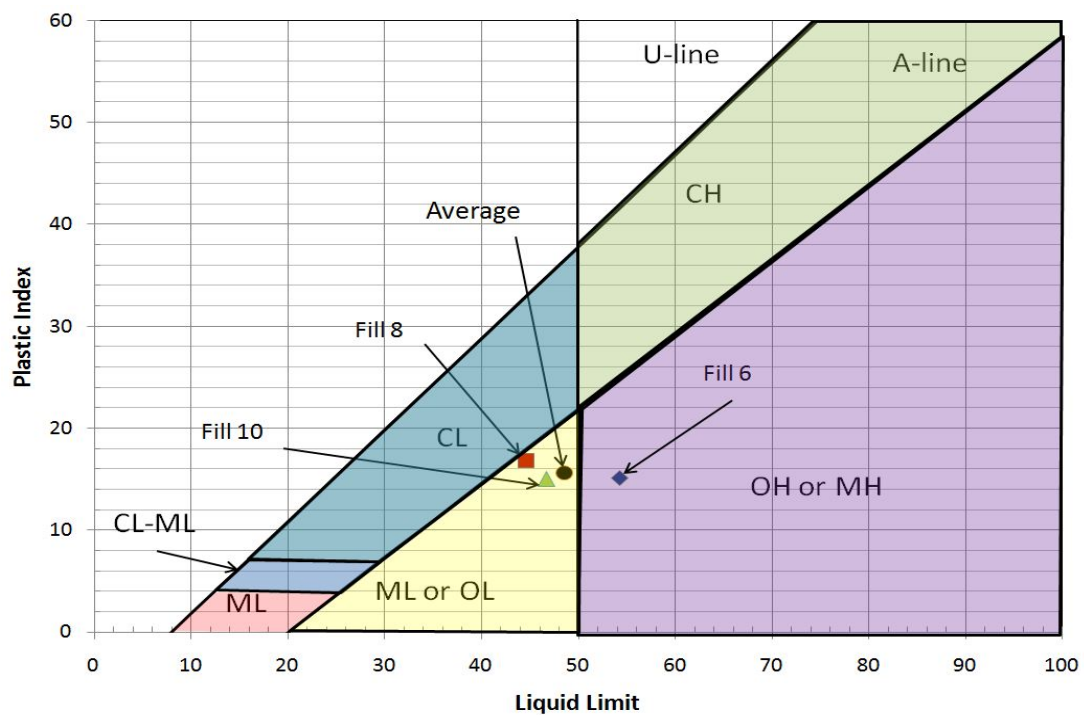


Figure 18. Plasticity chart for Fill 6, 8, and 10

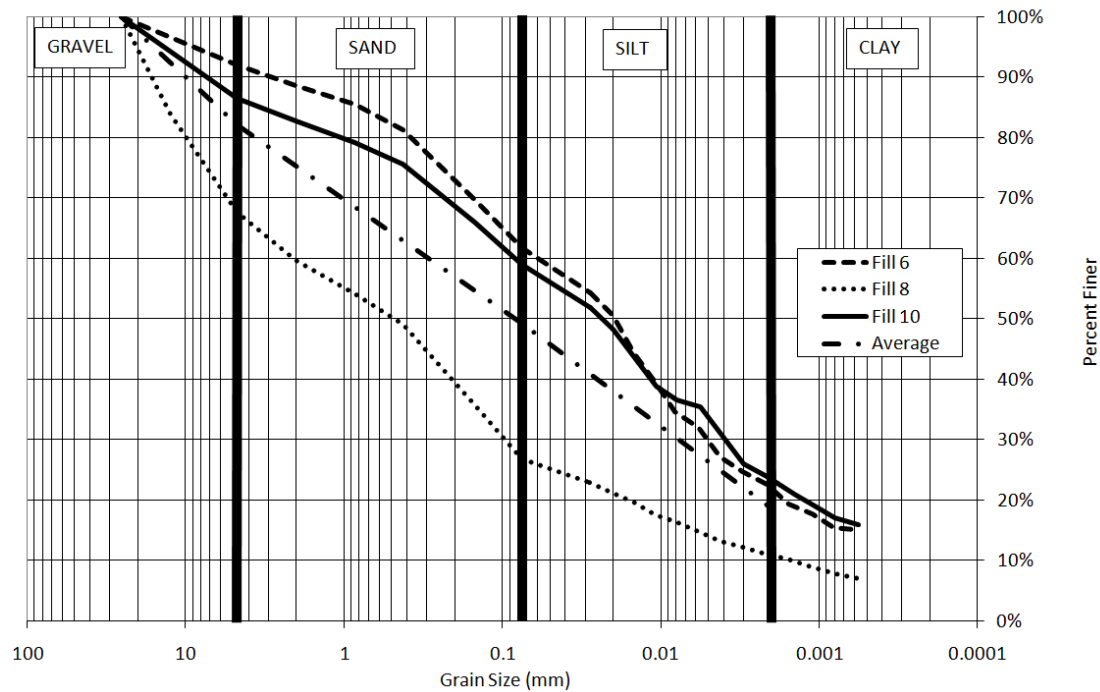


Figure 19. Grain size distribution plot for Fills 6, 8, 10

4.3.2 Standard and Modified Compaction Test

The maximum dry unit weight of each soil, in accordance to the standard compaction test (ASTM D698), was 92.9 pcf (14.6 kN/m³) at a water content of 25%. This corresponds to a moist unit weight of 116.5 pcf (18.3 kN/m³) on the project site. Soil compaction quality control data for Fill 6 was provided by Granite and compared with lab results. Our results appear to correlate well with quality control values from Granite Construction (Table 5). From the modified compaction test, the maximum dry unit weight was 103 pcf (16.2 kN/m³) with an optimum water content of 19%. The standard and modified compaction values can be seen in Figure 20.

Table 5. Standard compaction test data and comparison

Compaction Data					
Granite Construction (Fill 6 QC data)					
	Units	Wet Density	Dry Density	%WC	Percent Compaction
Average	(pcf)	116.2	94.1	24	100
	(kN/m ³)	18.2	14.8	24	100
Maximum	(pcf)	129.8	112.5	36	109
	(kN/m ³)	20.4	17.7	36	109
Minimum	(pcf)	105.6	79	11	91
	(kN/m ³)	16.6	12.4	11	91
OSU Lab (Fill 6 data)					
		Wet Density	Dry Density	%WC	
	(pcf)	116.2	92.9	25	
	(kN/m ³)	18.3	14.6	25	

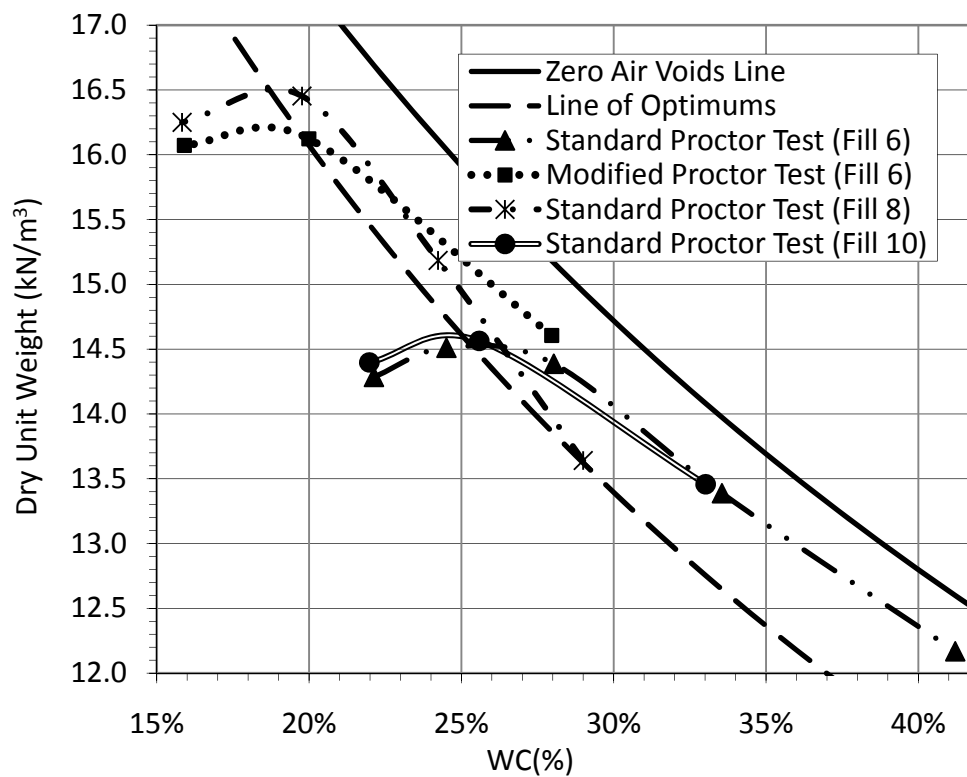


Figure 20. Standard and Modified Compaction Test Results

Note that the higher compactive effort produced by the modified compaction test allows the soil to be compacted at a lower water content and to a higher density. This, in turn, would lead to higher strength and a greater friction angle.

4.3.3 Consolidated – Undrained Triaxial Test

From the consolidated undrained (CU) test, an effective friction angle (ϕ') and effective cohesive strength (c') were found. The effective stress of a soil equals the total stress minus the pore water pressure within soil. For a consolidated undrained triaxial compression test, the pore pressures were recorded while total stress changed with increasing load and effective cell pressure remained constant. Because water cannot resist any force applied on it (i.e. has no shear strength) and it is not allowed to drain from the sample, all load applied is transferred to the soil specimen until the soil cannot hold the load, slips, and creates a shear failure plane. The difference in principal stresses is recorded at this point as well as the ratio of the major and minor principle stress. The difference is represented as the diameter of a Mohr's Circle, as shown in Figure 2. Each circle represents one triaxial compression test performed and, again, a Mohr-Coulomb failure envelope is placed tangent to all circles. The failure envelope is represented by the following equation:

$$\tau'_{ff} = \sigma'_{ff} \tan(\phi') + c' \quad (\text{Eq. 5})$$

which relates the effective shear stress at failure on the failure plane (τ'_{ff}) to effective normal stress at failure on the failure plane (σ'_{ff}), the effective friction angle

(ϕ') and the effective cohesive strength (c'). The effective shear strength at zero effective shear stress is the effective cohesive strength. Graphically, this is represented by Figure 21. Using this equation and testing completed, the effective friction angle (ϕ') found was 33.7° with an effective cohesive strength (c') of 18 kPa. The total stress parameters found were a total friction angle (ϕ) of 29° and a total cohesion (c) of 22 kPa.

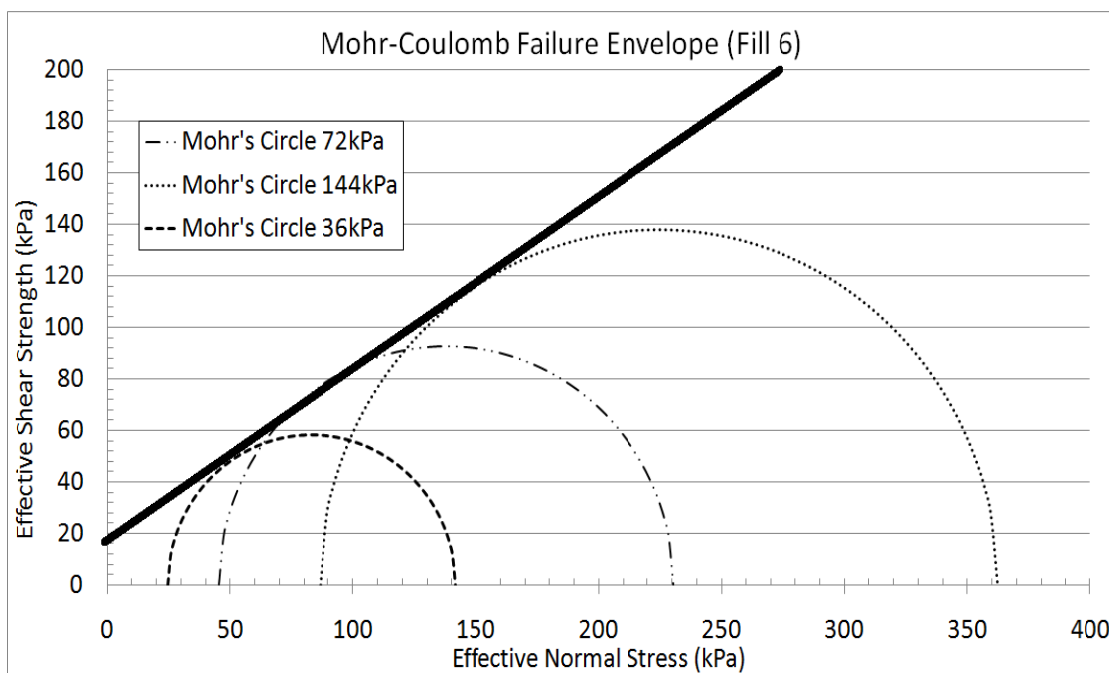


Figure 21. Approximate Mohr-Coulomb failure envelope from CU test (Fill 6)

4.3.4 Hydraulic Conductivity

The fill soil's hydraulic conductivity was, on average, approximately $1\text{E-}6$ in/s ($2.55\text{E-}6$ cm/s). Using Figure 7.7 in Holtz, Kovacs & Sheahan (2010), this value plots in the poor drainage soils area and can be characterized as a very fine sand, organic and inorganic silt, and/or a mixture of sand, silt, and clay. Given the soil characteristics in Figure 19, the soil tends toward the mixture of sand, silt and clay. Using the same figure

in Holtz, Kovacs & Sheahan (2010), this soil is characterized also as an impervious soil which can be modified by the effect of vegetation and weathering. The conductivity also indicates the soil is a silty sand (Todd & Mays, 2005), which, again, compares well with Figure 19.

4.3.5 Swell Test

The percent swell of the soil, in terms of the one-dimensional swell test, was approximately 6% which signifies a medium swelling potential (Seed, et. al., 1962). Since the plasticity index for the soil, on average, is approximately 16% and, analyzing the gradation curves, the soil has a medium degree of expansion [(Holtz W. G., 1959); (US Bureau of Reclamation, 1974)]. This medium expansion is primarily due to the amount of soil (15%) below 1 μ m.

During the free swell test, the soil increased in volume by approximately 15%. Although this is a marked increase compared to the one-dimensional swell test, soils with free swells less than 50% have been found to exhibit only small volume changes (Holtz, Kovacs, & Sheahan, 2010). Because of the results found from both tests, it was assumed that desiccation cracking would not occur on the fill slope due to the expansion and contraction of the soil.

Chapter 5: Numerical Slope Stability Modeling

5.1 Limit Equilibrium Slope Stability Modeling

5.1.1 Overview

Slope stability modeling was performed using a numerical analysis package, Slope/W. Slope/W was first created in 1977 as a tool to analyze the stability of earth structures through numerical analysis using many limit equilibrium methods (e.g. Ordinary method of slices, Janbu's Simplified Method, Bishop's Simplified Method, Spencer's procedure and the Morgenstern and Price procedure).

Slope/W evaluates slope stability using each method for a given soil slope model and calculates the factor of safety against slope failure for a set number of iterations assigned by the user. As was discussed in Chapter 1, an FS greater than one would be considered stable, less than one unstable and equal to one is considered at the equilibrium limit. For slopes of dams, levees, dikes, and other embankments and excavation slopes the US Army Corps of Engineers' Slope Stability Manual requires a 1.3 factor of safety for end of construction; 1.5 for long-term steady seepage; and 1.0-1.2 for rapid drawdown of pore water pressures (USACE, 2003).

For our analyses, the Morgenstern-Price procedure was selected. Of the three analyses that compute moment equilibrium (e.g. Bishop's, Ordinary, and Morgenstern - Price), Morgenstern – Price calculated, in general, the middle value of the three methods. For a more in depth comparison of these methods see (Duncan & Wright, 2005).

Slope/W performs a limit equilibrium slope stability analysis. Unfortunately, there are some limitations with the limit equilibrium procedure and with Slope/W, in general. Given that Slope/W is a limit equilibrium analysis program, all computations are based

solely on static conditions. Therefore, no analysis is done on displacements or strains within the soil structure while it is built and a more complete analysis of the soil slope's dynamics is created by finite element analysis programs.

5.2 Limit Equilibrium Slope Stability Modeling Procedure

In the Slope/W models, straw wattles were placed in 25 ft and 75 ft spacing along the slope of the fill to replicate on-site conditions. These straw wattles were constructed as point loads, considering the program operates in 2D modeling. The point load weight was based on a 2 meter cross section of straw wattle because many of the bracketed failures were typically 2 m wide. Slope/W performs many calculations of potential failure circles and their factors of safety using the methods described above. The potential slip circles that these methods calculate are centered in the grid shown in Figure 22. Multiple slip circles are generated from these centers creating several different potential failures for one embankment fill scenario. These failure circles can range from shallow to deep in depth.

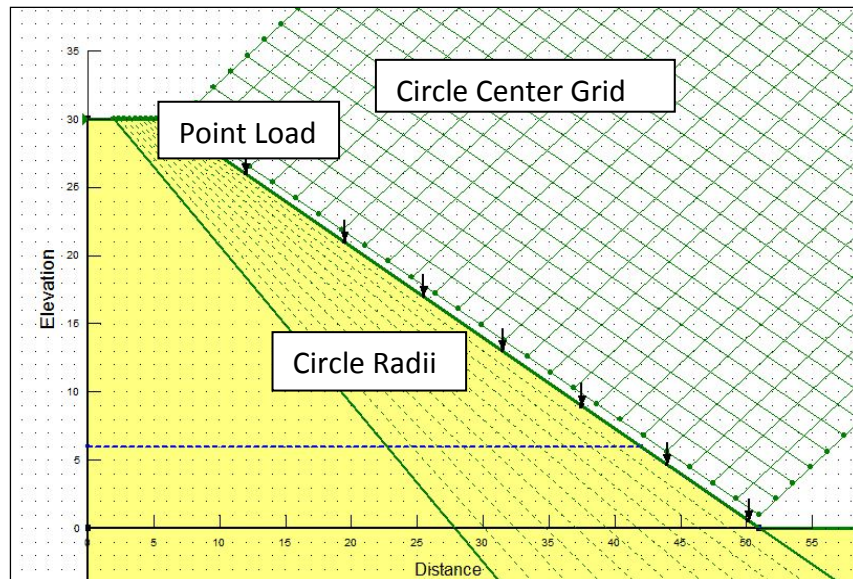


Figure 22. Slope/W slope model 1.5H:1V slope ratio

Each wattle was considered fully saturated based on on-site observations at time of failure and from straw wattle testing. Because many of the straw wattles were installed into the slope by excavating two to three inches of fill and driving a stake into the slope, several wattles appeared to be covered with soil. Therefore, a used straw wattle weight of 7.57 lbs (0.0337 kN) was used. Fill slopes were also modeled without straw wattles.

The soil and slope properties determined from testing and LiDAR investigation, including slope angle, slope height, and straw wattle spacing were entered into the software program and slope stability was analyzed.

A friction angle of 33.7 degrees was used, however, a cohesion value of zero kPa was assumed instead of the 18 kPa found during CU triaxial testing. As stated previously, the strength parameters from CU tests for gross stability overestimate soil cohesion (Day, 1994).

Also, if we use Equation 1 (rewritten below for convenience) with the fill slope angle ($\alpha = 33.7^\circ$), the soil friction angle ($\phi' = 33.7^\circ$), depth of failure ($D = 0.6$ to 0.9 m), total soil unit weight ($\gamma_t = 18.3$ kN/m³) and unit weight of water ($\gamma_w = 9.81$ kN/m³) found from triaxial tests and LiDAR investigations and back calculate the cohesion value (c') using an FS = 1, the cohesion value ranges from 2.6 to 4.2 kPa. These values are far less than that found in the CU test, validating our assumption that there was little to no cohesive strength in the soil when the slope failure occurred, or when $FS \leq 1$.

$$FS = \frac{c' + (\gamma_t - \gamma_w)D \cos^2(\alpha) \tan(\phi')}{\gamma_t D \sin(\alpha) \cos(\alpha)} \quad (\text{Eq. 1})$$

Multiple inclination angles were modeled by varying the slope ratio from 1H:1V to 1.5H:1V to 2H:1V. Based on the values found from standard compaction tests and the values given by Granite Construction, a moist unit weight of 18.3 kN/m³ was used for each slope embankment for Slope/W. It should be noted that the strength parameters (ϕ' , c') were based off samples compacted to the 18.3 kN/m³ moist unit weight. Had the soil been compacted to higher densities, (i.e. using the modified compaction test) strength in the soil and the friction angle would increase. This, in turn, would lead to higher factors of safety against slope failure using Equation 1.

5.3 Seepage and Climate Modeling

5.3.1 Overview

Vadose/W has the capacity to model the effect of many environmental factors on a fill slope. These include fluctuations in temperature, humidity, wind speed, and precipitation. Vegetation can also be modeled in this program. When these factors and

this modeling is coupled with Slope/W, a more comprehensive model can be created mimicking field conditions for surficial slope failures.

Vadose/W runs finite element seepage analysis in both steady-state and transient analyses by introducing vegetation and climate variables. The differences between the two are that steady-state analysis does not include changes in climate conditions while transient does. Because of this fact, a transient coupled model was completed for our analysis. Through coupled analysis, climate variables were also allowed to depend on each other (i.e. temperature depends on wind speed, relative humidity depends on rainfall, etc.) and were varied in a sinusoidal manner.

5.3.2 Seepage and Climate Modeling Procedure

To create a reliable model in Vadose/W, multiple parameters from the soil were needed including, hydraulic and thermal conductivity. These values were taken from Table 4.1 (Arya, 2001) for a saturated clay material. Also, general vegetation parameters, including root depth, were entered into the model. Given that much of the failed material showed grass root depths of 6 inches, this depth was used.

Climate data was also gathered and input into Vadose/W. Rainfall data from 2007 to 2010 from the project site was recorded and provided by Granite. For other variables, including temperature, relative density and wind speed, values were recorded from the KORTOLED4 weather station located in Toledo, OR approximately sixteen miles from the project site. This data was logged by staff from the website Weather Underground, developed in 1995 (Weather Underground Inc, 2011).

Because many surficial failures occurred in the wet season, data was collected for each month (October – April). To showcase the effect of rainfall, the months of least and most precipitation were entered into the program. From data given by Granite, these months were April 2009 and January 2008, respectively.

5.4 Modeling Results

5.4.1 Surficial Slope Failure Formation

The following sections discuss the factor of safety concerning different factors and the overall results of each are summarized.

5.4.2 Impact of Straw Wattles

From all programs used and models created, straw wattle weights seem to have little to negligible impact on slope stability. Various slope ratios, straw wattle spacing, fill heights and weights of straw wattles were considered in this analysis. These factors can be seen in Table 6 which shows the resulting factors of safety against slope failure for each model in the Slope/W program without on-site environmental conditions. Considering all these factors, straw wattles and their spacing widths are insignificant in comparison to the effects of slope ratio on a fill's factor of safety. Although there is some small difference in the values between 25 foot to 75 foot spacings, straw wattles, again, do not affect a slope's stability to any significant effect.

Table 6. Slope/W factors of safety for 30 and 40 meter tall fills without Vadose/W

30 METER TALL FILL				40 METERS TALL FILL			
Saturated Straw Wattle w/out Soil				Saturated Straw Wattle w/out Soil			
18.3 Moist UW				18.3 Moist UW			
SLOPE	Spacing			SLOPE	Spacing		
	No Watt.	25ft	75ft		No Watt.	25ft	75ft
1:1	0.680	0.680	0.680	1:1	0.680	0.680	0.680
1.5:1	1.017	1.018	1.017	1.5:1	1.017	1.017	1.017
2:1	1.358	1.358	1.358	2:1	1.353	1.353	1.353
Saturated Straw Wattle w/ Soil				Saturated Straw Wattle w/ Soil			
18.3 Moist UW				18.3 Moist UW			
SLOPE	Spacing			SLOPE	Spacing		
	No Watt.	25ft	75ft		No Watt.	25ft	75ft
1:1	0.680	0.680	0.680	1:1	0.680	0.680	0.680
1.5:1	1.017	1.018	1.017	1.5:1	1.017	1.017	1.017
2:1	1.358	1.358	1.358	2:1	1.353	1.353	1.353

These factors of safety, however, were the lowest found for each scenario, which may not necessarily be the same slip circle for each scenario. To directly investigate the relationship between slope stability and straw wattles, the 100 most critical slip failure circles were generated from Slope/W on a 1.5H:1V slope on a factor of safety map.

This safety map plots possible failure circles within the slope for each scenario analyzed. This map labels circles closer toward the model surface as areas with low factor of safety and circles deep in the models depth as areas with higher factor of safety. The difference in shades in between is 0.01 in the factor of safety value. An example of this is shown in Figure 23. From this figure, many of the more probable slope failures occur toward the top of the slope. This tendency towards failure at the top does not correlate well with the failures observed on-site where most failures are observed at the bottom of the slope. This may be because Slope/W is designed to evaluate existing slopes and does not take into account staged construction, which creates additional loading on the bottom of the slope. Also, Slope/W alone does not account for environmental factors,

which could very well influence where failure circles could occur on the slope. It was also noted that the factor of safety map at the top of the slope did not vary much with the straw wattle spacing scenarios. However, the bottom of the slope showed a slight decrease in factor of safety against global slope failure with no straw wattles.

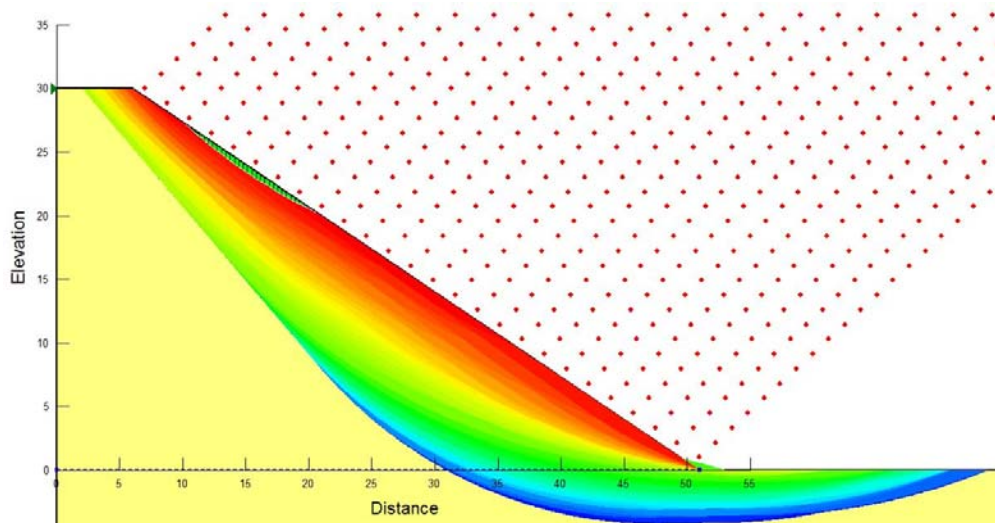


Figure 23. Factor of safety map against slope failure

These models varied straw wattle installation by increasing the spacing from 25 ft to 75ft to, eventually, no straw wattle installation. Each slip circle's factor of safety was compared with the same circle for the other scenarios. If there was a discrepancy between the two factors of safety, it was noted.

Of the 100 most critical slip surfaces, 98 were common between the no straw wattle and 25 foot straw wattle spacing scenarios. From this, 17 showed an increase in factor of safety of 0.001, 21 showed a decrease in factor of safety of 0.001, and 60 showed no change. The majority of the increases in factor of safety were due to a straw wattle located at the base of the failure circle resisting the force created by the soil mass

mobilization from the failure circle. In contrast, a decrease in the factor of safety was due to a straw wattle on the upper section of a failure circle adding weight to the mobile soil mass creating a failure circle. It should be said, however, these added weights are much smaller than the overall weight of the failed surface, hence, only a small increase and decrease of the factor of safety was seen.

The majority of these critical slip circles (86) occurred on the upper half of the slope. However, investigation of the factor of safety map showed a slight decrease in global stability at the bottom of the slope with 25 foot straw wattles as shown in Figure 24 and Figure 25. In both figures, the highest factor of safety against slope failure is toward the bottom of the model while the lowest factor of safety is shown at the slope's surface. The slight decrease in factor of safety, discussed earlier, is shown by a lack of the darker shade toward the bottom of the model in Figure 25. However, overall, the factor of safety against global failure was greater than 1 for all critical slip circles therefore slope failures at deeper depths are not possible with the variables considered.

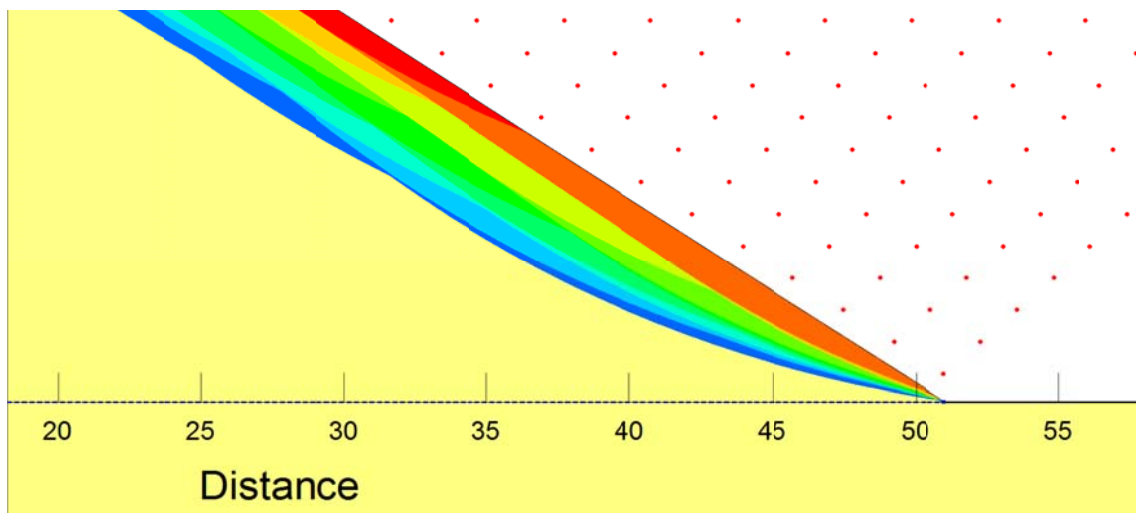


Figure 24. Factor of safety map for scenario with no straw wattles. Shades toward the surface represent decreased stability; shades toward the bottom represent increased stability.

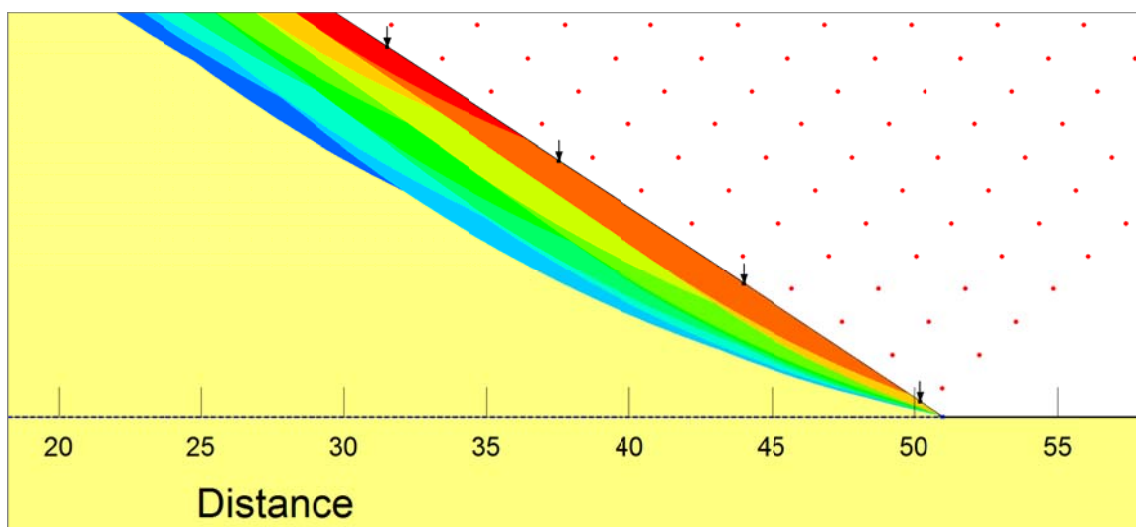


Figure 25. Factor of safety map for scenario with 25 ft straw wattle spacing. Note that the darker shade at the bottom disappears at the bottom of the slope compared to Figure 24.

When incorporating Vadose/W modeling into the Slope/W program, there is, again, a slight difference when straw wattles are installed. These results can be seen in Appendix CD. In these models, 366 scenarios were run. These scenarios incorporated

differences in slope ratio and straw wattle spacing with rainfall, humidity, temperature, and wind speed data. Of the 366, approximately 26 percent showed a difference when straw wattles were installed. 14 percent showed an improvement in slope stability while 12 percent showed a decrease. Again, these differences were often miniscule, showing an average difference of approximately 0.006 in factor of safety with a median value of 0.004. Given such small values, straw wattle weight appears to have a negligible effect on the stability of a fill slope.

5.4.3 Impact of Groundwater

Varying groundwater heights and straw wattle spacings were also analyzed in the Slope/W program. In the field, water was observed at approximately 18 meters below the ground surface of a natural slope. For our analysis, a 30 meter high 1.5H:1V fill slope was modeled with 18 m, 21 m, 24 m, 27 m, and 30 m ground water depths. If our y-axis datum is applied at the toe of the slope, these groundwater heights would be 12 meters, 9 meters, 6 meters, 3 meters, and zero meters.

Table 7 indicates that with an increase in groundwater height, the factor of safety against slope failure decreases substantially. Also, the probable area that these failures would occur is around the toe of the slope (0 m). These failures model the failure locations more closely than when no groundwater was used in the previous Slope/W modeling.

Given the factors of safety from Slope/W, the increase in groundwater height greatly decreases the factor of safety against slope failure and alludes to a much deeper failure than one that is surficial. While this is beneficial to understanding slope failures in

relation to groundwater, few depths seem to fit well with observations from US20PME. From LiDAR investigations, the volume of failed soil was 212 ft³ (6.5 m³). If we compare this value with Table 7, there was likely groundwater at the bottom of the slope. Also, the depths of failure (0.6 and 0.9 m) correlate well with a water table at the toe of the slope. Therefore, it is likely that the groundwater was at the toe of the slope during these surficial failures

Concerning straw wattles and their effect on the factor of safety, the wattles seem to slightly increase (approximately 0.001) the factor of safety. To show this increase, the same failure circle was compared with different straw wattle spacing. Figures 26-28 show a specific failure circle with such an increase in the factor of safety. These increases, however, are negligible.

Table 7. Factors of safety from critical slip surfaces with varying groundwater levels for 30m high fill with 1.5H:1V slope

Water Level (above Toe of Slope) (m)	~Depth of Failure (m)	Factor of Safety	Straw Wattle Spacing (ft)	Where on Slope (y-axis) (m)	Total Volume (m ³)
0	0.45	1.013	25	27.1	7.44
3	1.25	0.548	25	4.1	11.70
6	1.19	0.341	25	6.47	18.07
9	1.11	0.255	25	9.59	19.51
12	1.10	0.253	25	11.5	28.25
0	0.46	1.013	75	27.2	7.44
3	1.26	0.544	75	4.1	11.70
6	1.29	0.340	75	6.47	18.07
9	1.14	0.271	75	9.93	26.96
12	1.10	0.252	75	11.5	28.25
0	0.48	1.013	None	27.2	7.44
3	1.26	0.544	None	4.09	11.70
6	1.18	0.340	None	6.46	18.07
9	1.13	0.270	None	9.94	26.96
12	1.14	0.252	None	11.5	28.25

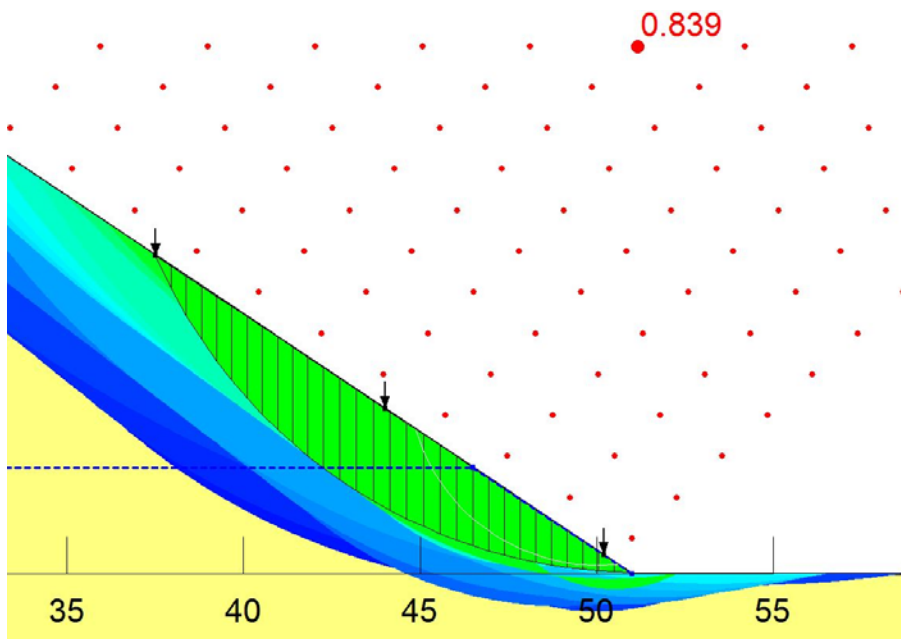


Figure 26. Failure circle with 25ft straw wattle spacing, 3m high water table

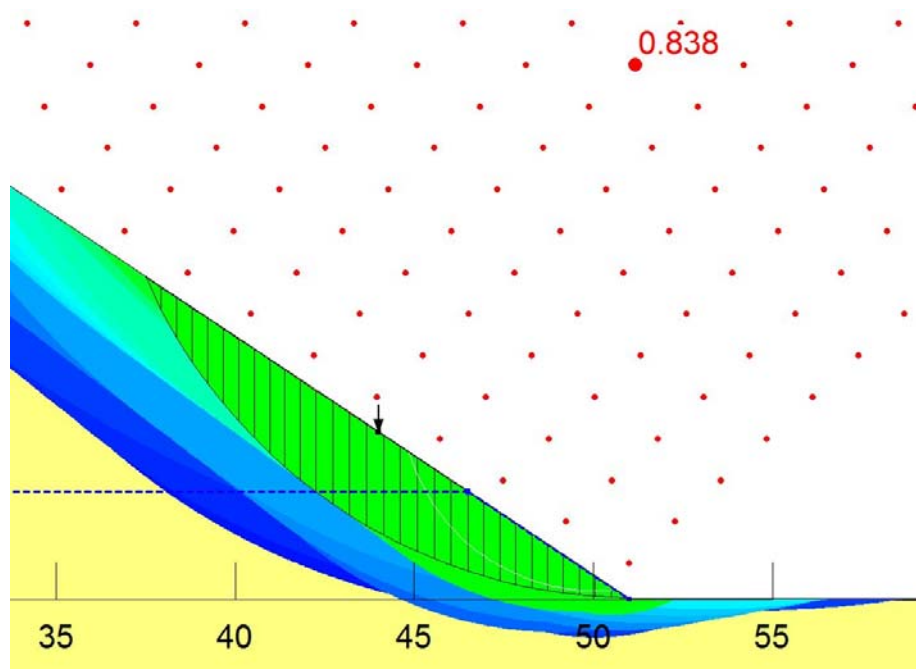


Figure 27. Failure circle with 75 ft straw wattle spacing, 3 m high water table

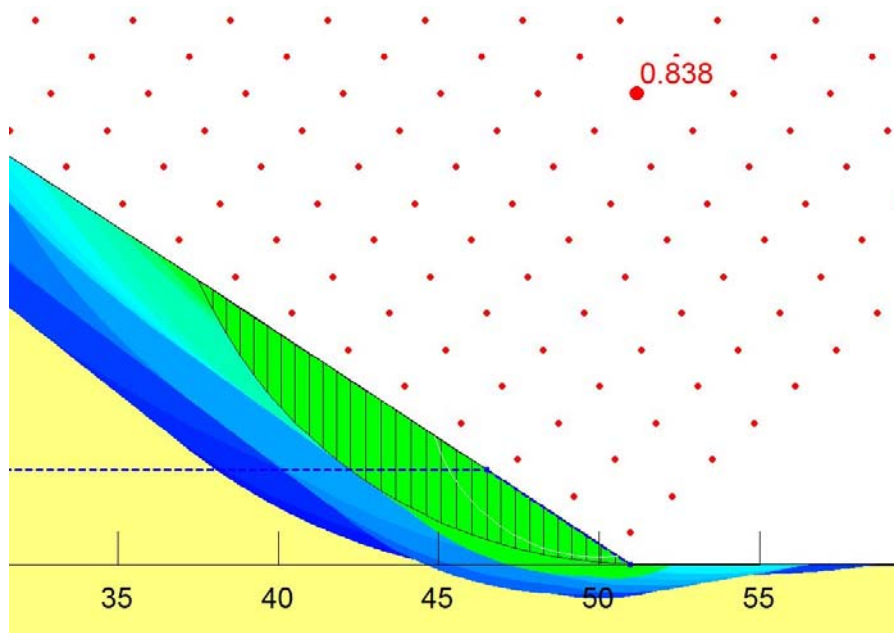


Figure 28. Failure circle with no straw wattles, 3m high water table

Overall stability modeling using $\phi' = 33.7^\circ$ and $c' = 18\text{kPa}$ (full cohesion) show that deep failures are unlikely, with or without straw wattles, unless there is a significant rise in groundwater.

5.4.4 Impact of Climate

Preliminary modeling suggests there is a significant change in factor of safety with rainfall and possibly temperature as seen in Figures 29-31. A dramatic increase in factor of safety at day 12 (Figure 30) is observed following the initial rainfall. The subsequent rainfall appears to have minimal effect on the factor of safety, until 2 inches of rainfall is seen on day 28. This may, perhaps, indicate that the rainfall below a threshold of 1 in. per day is required to lower the factor of safety. Further research is needed to verify this and additional impacts of rainfall, temperature and other environmental factors on slope stability.

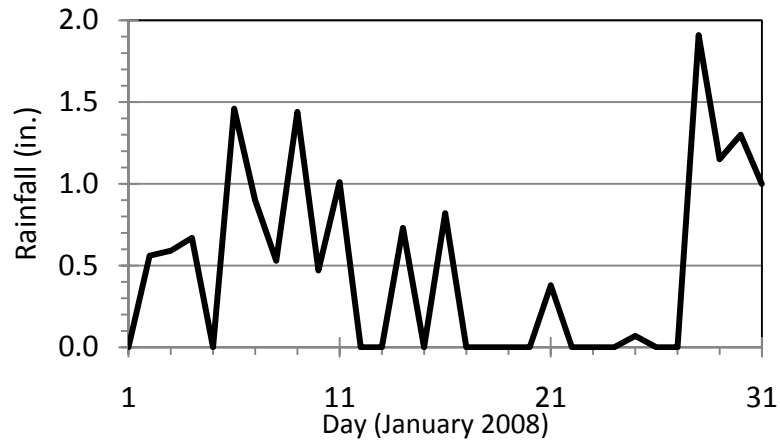


Figure 29. January 2008 rainfall

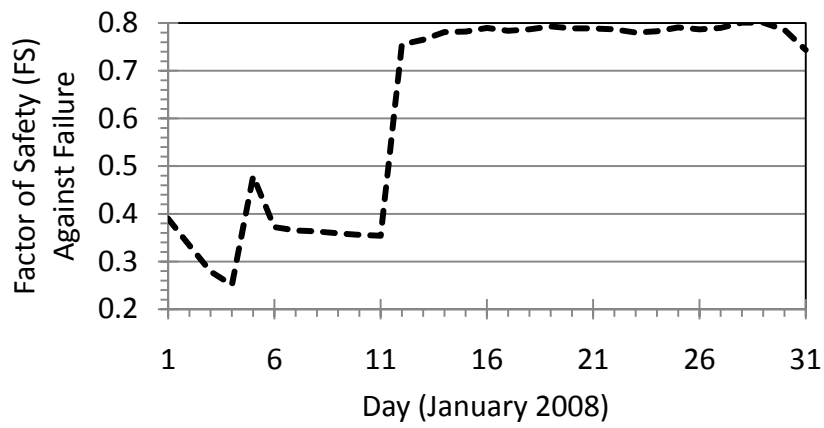


Figure 30. Slope /W with Vadose/W results

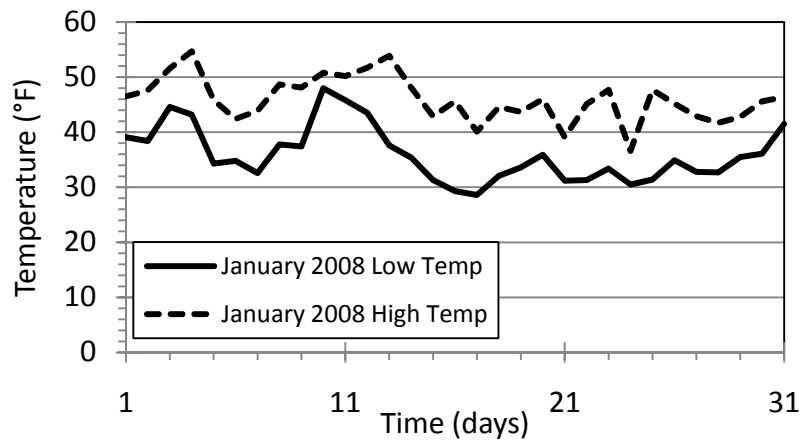


Figure 31. January 2008 temperature

Chapter 6: Conclusions and Recommendations

6.1 Conclusions

Several hypotheses were developed regarding the effect of straw wattles on slope stability, which were analyzed through LIDAR analysis, laboratory testing and slope stability modeling in this thesis:

1. Do straw wattles back up water on the slope, due to discrepancies in installment elevation, causing increased load and failure?
2. Do straw wattles add weight to the embankment slope, causing a surficial failure?
3. Do straw wattles prevent deeper failures from occurring?

The first hypothesis was disproven by verifying that the straw wattle elevations followed the slope contours using LiDAR analysis. Therefore, it is unlikely that water collected at low points in the straw wattle adding more weight to the fill slope causing a surficial failure. Also, LiDAR measurements determined several parameters including fill height, slope angle, straw wattle spacing, depth of surficial failure, and volume of soil failed. In general, the slopes of each fill were 1.5H:1V with fill heights ranging from 30 to 40 meters. Straw wattle spacing was approximately 25 feet and each failure depth observed was surficial in nature (2 to 3 feet (0.6 to 0.9 m)).

From the lab tests completed, the on-site soil has a friction angle (ϕ') of 33.7° and a cohesion limit (c') of 18 kPa. However, for our modeling, it was assumed that the cohesion limit was zero kPa. Through back calculation, using Equation 1 and LiDAR analysis, the true cohesion value ranged from 2.6 to 4.2 kPa. This difference is

considerable and adds credibility to our assumption that the cohesion limit was near zero when the surficial slope failure occurred.

Several numerical models were analyzed using variations in slope angle, straw wattle spacing, and climate conditions. From those results, very little change in factor of safety against surficial and deep slope failures was observed with varying straw wattle spacing (0.006 on average). Also, these differences were miniscule when compared to the effects of slope angle, climate conditions, and likely soil variability. Because of these very small changes, we can conclude that there is no significant relationship between straw wattle placement and slope stability, surficial or otherwise, disproving the second and third hypotheses.

6.2 Recommendations

Given that there is negligible effect to the slope stability, straw wattles can continue to be applied at a constant elevation along the slope, provided they are properly installed. However, this recommendation specifically concerns slope stability and the optimum placement of straw wattles to curb soil erosion should be consulted with erosion control professionals.

To prevent surficial failures in the future, many different devices can be used. Biotechnical stabilization procedures can be used by alternating brush layers incorporated into the fill with compacted soil. These layers reinforce the fill and also act as horizontal drains in the slope (Gray & Sotir, 1992). These devices are also cost effective and do not cause much site disturbance (Gray & Sotir, 1992). Another conventional solution includes installing a rock blanket over the fill slope. Since many of the slope failures

were 1 to 2 ft in depth, vegetation with deeper root lengths, as discussed by Day (1993), will improve slope stability. Subgrade geotextile below the root depth can increase the shear friction between two soil masses, again, decreasing the likelihood of a surficial slope failure. Day (1996) also discusses other repair methods.

Examining Table 6, one can easily assume that lowering the slope angle can increase the factor of safety against surficial slope failure. Unfortunately, this does not take into account the availability of right-of-way land or the requirements for certain structures in a project (i.e. overpasses, bridges, etc.). Yet, if right-of-way land is attainable, decreasing the slope angle would be a recommendation.

Another precaution would be to use the optimum density and moisture content from the modified compaction test rather than the standard proctor test. The modified compaction results, as seen in Figure 20, show that the maximum dry density is increased and the optimum moisture content is decreased. This increase in density causes the soil's friction angle to increase as well, which then increases the strength of the soil material. Also, when compacted at a lower optimum moisture content, the soil is further from the liquid limit, resulting in more stability.

Vegetation plays a major part in the slope's stability. Since increasing root depth in a soil increases the strength of the soil, implementation of vegetation with deeper root depths will improve surficial slope stability. This does not only increase the strength of the soil but may decrease the moisture content of the soil due to evapo-transpiration and precipitation blocking from trees, bushes, etc. Therefore, especially in concert with the

application of modified compaction values, more rainfall would be needed to cause the soil to reach its liquid state, where no strength is apparent.

Finally, significant rainfall can lead to slope instability in spite of the above noted treatments. With rainfall penetration, the soil's cohesion reduces to near zero causing its overall strength near the surface to reduce to zero. Rainfall also adds more weight to a slope fill, which, when looking at the US20PME case study, for example, could have some detrimental effects, given that the slopes are at the limit of equilibrium. Therefore, climate conditions should always be taken into account when designing and constructing fill slopes.

6.3 Future Evaluation

The insights obtained through this research present several additional questions. First, the progression of the failures is of interest. Unfortunately, insufficient history of failure progression and inability to observe any failures during the study period did not allow for such study. Additional evaluation through high resolution 3D modeling using LiDAR can produce time-series spatial data to show the progression of failures. Also, it can provide accurate volume estimates of the failure masses. We have conducted a few LiDAR surveys at specific locations at US20PME and will continue to perform these surveys, as necessary.

As a recommendation to all job sites, failures should be documented both temporally and spatially. More spatial data recording including size of failed slide, date of slide, spatial location, etc. would immediately enhance our understanding of failure progression and the mechanisms affecting surficial slope failures. Also, with more

density testing location data, surficial failures and compaction locations could be correlated and an evaluation could be made relating compaction density and probability of surficial slope failure.

Increased slope and seepage modeling will provide insights into fluid flow around a straw wattle. This will also give more insight into the dynamics of where the water is seeping into the fill slope and whether such seepage (and subsequent forces) is a significant failure mechanism; and, if so, this may provide insight into where the failure surface initiates. More analyses could be performed at a finer scale to evaluate the critical slope angle where straw wattles tend to produce only a positive impact versus only a negative impact on slope stability. In this study, 1H:1V, 1.5H:1V, and 2H:1V slopes were evaluated, while other permutations of evaluation may expose interesting relationships. Development of an experimental test bed to simulate field failures could be used to investigate this critical threshold.

Given that the modified compaction test yields a higher maximum dry density and lower optimum moisture content, more triaxial testing using a sample compacted to a higher density is of interest to show the increase in strength. Also, an unconfined submerged triaxial test would be beneficial to understand the soil's true cohesion. Back-calculated values from additional failures observed will also be important to correlate field tests to lab tests.

BIBLIOGRAPHY

- Al-Homoud, A. S., Basma, A. A., Malkawi, A. H., & Al Bashabsheh, M. A. (1995). Cyclic Swelling Behavior of Clays. *Journal of Geotechnical Engineering* , 562-565.
- Arya, S. P. (2001). *Introduction to Micrometeorology*. New York: Academic Press, Inc.
- Bardet, J.-P. (1997). *Experimental Soil Mechanics*. Upper Saddle River: Prentice-Hall Inc.
- Bishop, D. M., & Stevens, M. E. (1964). *Landslides on logged areas, southeast Alaska*. Juneau: US Department of Agriculture.
- Cho, S. E., & Lee, S. R. (2002). Evaluation of Surficial Stability for Homogeneous Slopes Considering Rainfall Characteristics. *Journal of Geotechnical and Geoenvironmental Engineering* , 756-763.
- Clopper, P., Vielleux, M., & Johnson, A. (2001). Quantifying the Performance of Hillslope Erosion Control Best Management Practices. *World Water Congress* (pp. 1-10). Berlin: American Society of Civil Engineers.
- Cruden, D. M., & Varnes, D. J. (1996). Landslide Types and Processes. *Landslides: Investigation and Mitigation Special Report 247* , 36-75.
- Day, R. W. (1996, August). Design and Repair for Surficial Slope Failures. *Practice Periodical on Structural Design and Construction* , pp. 83-87.
- Day, R. W. (1999). *Geotechnical Engineer's Portable Handbook*. New York: McGraw-Hill Professional.
- Day, R. W. (1993). Surficial Slope Failure: A Case Study. *Journal of Performance of Constructed Facilities* , 264-269.
- Day, R. W. (1994). Surficial Stability of Compacted Clay: Case Study. *Journal of Geotechnical Engineering* , 1980-1990.
- Day, R. W., & Axten, G. W. (1990). Softening of Fill Slopes Due to Moisture Infiltration. *Journal of Geotechnical Engineering* , 1424-1427.
- Duncan, J. M., & Wright, S. G. (2005). *Soil Strength and Slope Stability*. Hoboken: John Wiley & Sons, Inc.

- Endo, T., & Tsuruta, T. (1968). The effect of the tree's roots on the shear strength of soil. *Annual Report* , 167-182.
- Evans, D. A. (1972). Slope Stability Report. *Slope Stability Committee*. Los Angeles: Department of Building and Safety.
- Fernandes, N. F., Netto, A. L., & Lacerda, W. A. (1994). Subsurface hydrology of layered colluvium mantles in unchanneled valleys -- south-eastern Brazil. *Earth Surface Processes and Landforms* , 609-626.
- Fujiwara, K. (1970). A study on the landslides by aerial photographs. *Res. Bull. Exp. Forest Hokkaido University* , 297-345.
- Gehling, C. (2010, April 10). Straw Wattle Installation and General Observations. (A. Rikli, Interviewer).
- Gray, D. H., & Sotir, R. B. (1992). Biotechnical Stabilization of Highway Cut Slope. *Journal of Geotechnical Engineering* , 1395-1409.
- Greenwood, J., Norris, J., & Wint, J. (2004). Assessing the contribution of vegetation to slope stability. *Geotechnical Engineering* , 199-207.
- Hammond, C. M., Meier, D., & Beckstrand, D. (2009). Paleo-landslides in the Tye Formation and highway construction, central Oregon Coast Range. *GSA Field Guides* , 481-494.
- Holtz, R. D., Kovacs, W. D., & Sheahan, T. C. (2010). *An Introduction to Geotechnical Engineering*. Upper Saddle River: Prentice-Hall, Inc.
- Kayen, R., Stewart, J. P., & Collins, B. (2010). Recent advances in terrestrial LIDAR applications in geotechnical earthquake engineering. *5th International Conference on Recent Advances in Geotechnical Earthquake Engineering and Soil Dynamics*. San Diego.
- Kelsey, H. M., Ticknor, R. L., Bockheim, J. G., & Mitchell, E. (1996). Quaternary upper plate deformation in coastal Oregon. *Geological Society of America Bulletin* , 843-860.
- Kelsey, K., Johnson, T., & Vavra, R. (2010). *Needed information: Testing, analysis, and performance values for slope interruption perimeter control BMPs*. Retrieved April 13, 2010, from International Erosion Control Association: <http://www.ieca.org/membersonly/cms/content/Proceedings/Object392PDFEnglish.pdf>

- Kim, Y. K., & Lee, S. R. (2010). Field Infiltration Characteristics of Natural Rainfall in Compacted Roadside Slopes. *Journal of Geotechnical and Geoenvironmental Engineering* , 248-252.
- Lambe, T. W., & Whitman, R. V. (1969). *Soil Mechanics*. New York: John Wiley & Sons.
- Maryland Department of the Environment Water Management Administration. (1999, September). MGWC 2.6: Natural Fiber Rolls. *Maryland Department of the Environment Waterway Construction Guidelines* . Maryland, USA: Maryland Department of the Environment Water Management Administration.
- Michalowski, R. L. (2000). Secondary Reinforcement for Slopes. *Journal of Geotechnical and Geoenvironmental Engineering* , 1166-1173.
- Michalowski, R. L. (2002). Stability Charts for Uniform Slopes. *Journal of Geotechnical Engineering* , 351-355.
- Montgomery, D. R., Dietrich, W. E., Torres, R., Anderson, S. P., Heffner, J. T., & Loague, K. (1997). Hydrologic response of a steep, unchanneled valley to natural and applied rainfall. *Water Resources Research* , 91-109.
- Natural Resources Conservation Service. (2009, 11 11). *Web Soil Survey*. Retrieved September 2010, from Natural Resources Conservation Service: <http://websoilsurvey.nrcs.usda.gov/app/WebSoilSurvey.aspx>
- Olsen, M. J., Johnstone, E., Kuester, F., Driscoll, N., & Ashford, S. A. (2011). New Automated Point-Cloud Alignment for Ground-Based Light Detection and Ranging Data of Long Coastal Sections. *Journal of Surveying Engineering* .
- Oregon Department of Transportation. (2008). 00280.16 Sediment Control Materials. In O. D. Transportation, *2008 Standard Specifications for Construction* (pp. 47-48).
- Osman, N., & Barakbah, S. (2006). Parameters to predict slope stability - Soil water and root profiles. *Ecological Engineering* , 90-95.
- Pradel, D., & Raad, G. (1993). Effect of Permeability on Surficial Stability of Homogeneous Slopes. *Journal of Geotechnical Engineering* , 315-332.
- Rahardjo, H., Ong, T. H., Rezaur, R. B., & Leong, E. C. (2007). Factors Controlling Instability of Homogeneous Soil Slopes under Rainfall. *Journal of Geotechnical and Geoenvironmental Engineering* , 1532-1543.

- Roering, J. J., Schmidt, K. M., Stock, J. D., Dietrich, W. E., & Montgomery, D. R. (2003, February 27). *Shallow landsliding, root reinforcement, and spatial distribution of trees in the Oregon Coast Range*. Retrieved April 2010, from NRC Research Press Web: <http://cgj.nrc.ca>
- Rogers, N., & Selby, M. J. (1980). Mechanisms of shallow translational landsliding during summer rainstorms: North Island, New Zealand. *Geografiska Annaler. Series A, Physical Geography* , 11-21.
- Ruhe, R. (1975). *Geomorphology*. Boston: Houghton Mifflin.
- Sidle, R. C., & Ochiai, H. (2006). *Landslides: Processes, Prediction, and Land Use*. Washington, DC: American Geophysical Union.
- Sidle, R. (1984). Shallow groundwater fluctuations in unstable hillslopes of coastal Alaska. *Z. fur Gletscherkunde und Glazialgeol.* , 79-95.
- Snively, J. P., Wagner, H. C., & MacLeod, N. S. (1964). Rhythmic-bedded Eugeosynclinal Deposits of the Tye Formation, Oregon Coast Range. *Kansas Geological Survey* , 461-480.
- Swanson, F., & Dyrness, C. (1975). Impact of clearcutting and road construction on soil erosion by landslides in the western Cascade Range, Oregon. *Geology* , 393-396.
- Trast, J. M., & Benson, C. H. (1995). Estimating Field Hydraulic Conductivity of Compacted Clay. *Journal of Geotechnical Engineering* , 736-739.
- Tsuboyama, Y., Sidle, R. C., Noguchi, S., Murakami, S., & Shimizu, T. (2000). A zero-order basin - its contribution to catchment hydrology and internal hydrological processes. *Hydrological Processes* , 387-401.
- University of West England, Bristol. (2010, December 17). *GeotechniCAL Reference*. Retrieved December 17, 2010, from University of West England, Bristol: <http://environment.uwe.ac.uk/geocal/foundations/foundations.htm>
- Van de Water, P., Leavitt, S., Jull, T., Squire, J., & Testa, N. (2009). *Tree Boles Revealed in Pacific Northwest Landslide Deposits Provide Tree-Ring Record for Period Prior to Deglaciation*. Retrieved July 2010, from US 20 Pioneer Mountain to Eddyville: <http://www.us20pme.com>
- Van De Wiel, M. J., & Darby, S. E. (2007). A new model to analyse the impact of woody riparian vegetation on the geotechnical stability of riverbanks. *Earth Surface Processes and Landforms* , 2185-2198.

- Varnes, D. J. (1978). Slope Movement Types and Processes. In T. R. Board, *Chapter 2: Landslides: Analysis and Control, Special Report 176* (p. 234). Washington, D.C.: National Academy of Sciences.
- Weather Underground, Inc. (2011). *Toledo, OR*. Retrieved November 2010, from Weather Underground: <http://www.wunderground.com/cgi-bin/findweather/getForecast?query=97391&sp=KORTOLED4>
- Wiley, T. J. (2000). Relationship between rainfall and debris flows in western Oregon. *Oregon Geology*, 27-47.
- Wu, T. H., Riestenberg, M. M., & Flege, A. (1994). Root properties for design of slope stabilization. *Proceedings of the International Conference on Vegetation and Slopes: Stabilization, Protection and Ecology*. Oxford.
- Yaquina River Constructors. (2008-2010). *US 20 Pioneer Mountain to Eddyville*. Retrieved April 2010, from US 20 Pioneer Mountain to Eddyville: <http://www.us20pme.com/>

APPENDICES

APPENDIX A: Site and Boring Properties

Table A-1 50G site and boring properties (Natural Resources Conservation Service, 2009)

<p>50G—Preacher-Bohannon-Slickrock complex, 35 to 60 percent slopes</p> <p>Map Unit Setting</p> <p>Elevation: 30 to 1,800 feet</p> <p>Mean annual precipitation: 60 to 110 inches</p> <p>Mean annual air temperature: 46 to 52 degrees F</p> <p>Frost-free period: 145 to 210 days</p> <p>Map Unit Composition</p> <p>Preacher and similar soils: 40 percent</p> <p>Bohannon and similar soils: 25 percent</p> <p>Slickrock and similar soils: 20 percent</p> <p>Description of Preacher</p> <p>Setting</p> <p>Landform: Mountain slopes</p> <p>Landform position (two-dimensional): Backslope</p> <p>Landform position (three-dimensional): Mountainflank</p> <p>Down-slope shape: Convex</p> <p>Across-slope shape: Convex</p> <p>Parent material: Colluvium derived from sedimentary rock</p> <p>Properties and qualities</p> <p>Slope: 35 to 60 percent</p> <p>Depth to restrictive feature: 40 to 60 inches to paralithic bedrock</p> <p>Drainage class: Well drained</p> <p>Capacity of the most limiting layer to transmit water (Ksat): Moderately high to high (0.57 to 1.98 in/hr)</p> <p>Depth to water table: More than 80 inches</p> <p>Frequency of flooding: None</p> <p>Frequency of ponding: None</p> <p>Available water capacity: Very high (about 12.9 inches)</p> <p>Interpretive groups</p> <p>Land capability (nonirrigated): 6e</p> <p>Typical profile</p> <p>0 to 3 inches: Slightly decomposed plant material</p> <p>3 to 18 inches: Loam</p> <p>18 to 48 inches: Clay loam</p> <p>48 to 57 inches: Loam</p> <p>57 to 67 inches: Weathered bedrock</p> <p>Description of Bohannon</p> <p>Setting</p> <p>Landform: Mountain slopes</p>
--

Landform position (two-dimensional): Backslope
Landform position (three-dimensional): Mountainflank
Down-slope shape: Convex, concave
Across-slope shape: Convex, concave
Parent material: Colluvium derived from sedimentary rock
Properties and qualities
Slope: 35 to 60 percent
Depth to restrictive feature: 20 to 40 inches to paralithic bedrock
Drainage class: Well drained
Capacity of the most limiting layer to transmit water (Ksat): High (1.98 to 5.95 in/hr)
Depth to water table: More than 80 inches
Frequency of flooding: None
Frequency of ponding: None
Available water capacity: Low (about 5.1 inches)
Interpretive groups
Land capability (nonirrigated): 6e
Typical profile
0 to 1 inches: Slightly decomposed plant material
1 to 17 inches: Gravelly loam
17 to 32 inches: Gravelly loam
32 to 42 inches: Weathered bedrock
Description of Slickrock
Setting
Landform: Mountain slopes
Landform position (two-dimensional): Backslope
Landform position (three-dimensional): Mountainflank
Down-slope shape: Concave, convex
Across-slope shape: Concave, convex
Parent material: Recent loamy colluvium derived from sandstone and siltstone over older fine-loamy colluvium derived from sandstone and siltstone
Properties and qualities
Slope: 35 to 60 percent
Depth to restrictive feature: 40 to 60 inches to paralithic bedrock
Drainage class: Well drained
Capacity of the most limiting layer to transmit water (Ksat): Moderately high to high (0.57 to 1.98 in/hr)
Depth to water table: More than 80 inches
Frequency of flooding: None
Frequency of ponding: None
Available water capacity: High (about 11.3 inches)
Interpretive groups

Land capability (nonirrigated): 6e
Typical profile
0 to 1 inches: Slightly decomposed plant material
1 to 15 inches: Gravelly loam
15 to 40 inches: Gravelly loam
40 to 54 inches: Very cobbly loam
54 to 64 inches: Weathered bedrock

APPENDIX B: Lab Test Data

Table B-1 Sieve analysis data for Fill 6

Sieve Analysis Fill 6						
Mass of Soil =		2032 g		200 Wash Mass =		1244.96 g
Sieve No	Sieve Opening (mm)	Mass Sieve (g)	Mass Sieve + Soil Retained (g)	Mass Retained (g)	Percent Retained (%)	Percent Passing (%)
1"	25.4	572.2	572.2	0	0.00%	100.00%
4	4.75	527.16	687.82	160.66	7.91%	92.09%
10	2	458.73	528.93	70.2	11.36%	88.64%
20	0.85	406.18	470.93	64.75	14.55%	85.45%
40	0.425	390.98	474.19	83.21	18.64%	81.36%
100	0.15	326.68	562.32	235.64	30.23%	69.77%
200	0.075	332.32	495.15	162.83	38.25%	61.75%
pan	-	372.14	382.2	1255.02	100.00%	0.00%
Total				2032.31 g		
Soil Lost				-0.31 g		

Table B-2 Sieve analysis data for Fill 8

Sieve Analysis Fill 6						
Mass of Soil =		2032 g		200 Wash Mass =		1244.96 g
Sieve No	Sieve Opening (mm)	Mass Sieve (g)	Mass Sieve + Soil Retained (g)	Mass Retained (g)	Percent Retained (%)	Percent Passing (%)
1"	25.4	572.2	572.2	0	0.00%	100.00%
4	4.75	527.16	687.82	160.66	7.91%	92.09%
10	2	458.73	528.93	70.2	11.36%	88.64%
20	0.85	406.18	470.93	64.75	14.55%	85.45%
40	0.425	390.98	474.19	83.21	18.64%	81.36%
100	0.15	326.68	562.32	235.64	30.23%	69.77%
200	0.075	332.32	495.15	162.83	38.25%	61.75%
pan	-	372.14	382.2	1255.02	100.00%	0.00%
Total				2032.31 g		
Soil Lost				-0.31 g		

Table B- 3 Sieve analysis data for Fill 10

Sieve Analysis Fill 10						
Mass of Soil = 2391.41 g			200 Wash Mass = 1399.92 g			
Sieve No	Sieve Opening (mm)	Mass Sieve (g)	Mass Sieve + Soil Retained (g)	Mass Retained (g)	Percent Retained (%)	Percent Passing (%)
1"	25.4	572.2	572.2	0	0.00%	100.00%
4	4.75	527.48	850.47	322.99	13.50%	86.50%
10	2	458.73	548.75	90.02	17.27%	82.73%
20	0.85	406.41	493.22	86.81	20.89%	79.11%
40	0.425	390.88	475.42	84.54	24.43%	75.57%
100	0.15	326.65	554.37	227.72	33.95%	66.05%
200	0.075	332.27	500.22	167.95	40.97%	59.03%
pan	-	372.17	384.32	1412.07	100.00%	0.00%
Total				2392.1 g		
Soil Lost				-0.69 g		

Table B- 4 Fill 6 liquid limit, plastic limit and plasticity index data

Liquid Limit				
Can No.	1	2	3	4
Mass of wet soil + can	20.17	19.25	18.04	16.19
Mass of dry soil + can	14.54	14	12.7	11.63
Mass of can	3.92	3.93	3.97	3.65
Mass of dry soil	10.62	10.07	8.73	7.98
Mass of moisture	5.63	5.25	5.34	4.56
Water content, w%	53.01%	52.14%	61.17%	57.14%
No. of taps, N	27	34	12	18
Plastic Limit				
Can No.	1	2	3	4
Mass of wet soil + can	6.08	6.25	10.97	6.49
Mass of dry soil + can	5.42	5.56	8.88	5.7
Mass of can	3.73	3.76	3.66	3.7
Mass of dry soil	1.69	1.8	5.22	2
Mass of moisture	0.66	0.69	2.09	0.79
Water content, w%	39.05%	38.33%	40.04%	39.50%

Table B- 5 Fill 8 liquid limit, plastic limit and plasticity index data

Liquid Limit				
Can No.	1	2	3	4
Mass of wet soil + can	17.42	14.91	13.88	15.15
Mass of dry soil + can	13.35	11.51	10.58	11.76
Mass of can	3.74	3.73	3.71	3.87
Mass of dry soil	9.61	7.78	6.87	7.89
Mass of moisture	4.07	3.4	3.3	3.39
Water content, w%	42.35%	43.70%	48.03%	42.97%
No. of taps, N	29	27	17	35
Plastic Limit				
Can No.	1	2	3	4
Mass of wet soil + can	5.53	6.83	6.19	N/A
Mass of dry soil + can	5.12	6.18	5.65	N/A
Mass of can	3.66	3.87	3.66	N/A
Mass of dry soil	1.46	2.31	1.99	N/A
Mass of moisture	0.41	0.65	0.54	N/A

Table B- 6 Fill 10 liquid limit, plastic limit and plasticity index data

Liquid Limit			
Can No.	1	2	3
Mass of wet soil + can	18.1	18.01	19.36
Mass of dry soil + can	13.69	13.27	14.41
Mass of can	3.82	3.63	3.76
Mass of dry soil	9.87	9.64	10.65
Mass of moisture	4.41	4.74	4.95
Water content, w%	44.68%	49.17%	46.48%
No. of taps, N	45	16	21
Plastic Limit			
Can No.	1	2	3
Mass of wet soil + can	6.62	6.95	6.1
Mass of dry soil + can	5.91	6.16	5.48
Mass of can	3.62	3.62	3.61
Mass of dry soil	2.29	2.54	1.87
Mass of moisture	0.71	0.79	0.62
Water content, w%	31.00%	31.10%	33.16%

Table B- 7 Standard compaction data for Fill 6

Standard Proctor Test (Fill 6)					
Mold Dimensions					
Height	11.7	cm	Diameter	10.2	cm
Volume	948.5564	cm ³			
Mass of Mold	4253	g			
Sample Label	9	7	5	3	2
Mass of cup, g	1.0	1.0	1.0	41.5	41.6
Mass of cup + wet soil, g	24.4	31.4	36.6	1757.0	1676.0
Mass of cup + dry soil, g	20.1	25.4	28.8	1326.0	1199.0
Mass of water, g	4.24	5.98	7.81	431	477
Mass of dry soil, g	19.16	24.4	27.86	1284.53	1157.42
Water content, w (%)	22.13%	24.51%	28.03%	33.55%	41.21%
Water content, w (%)	22.13%	24.51%	28.03%	33.55%	41.21%
Mass of soil + mold, g	5930.4	5990.0	6024.0	5972.0	5905.0
Mass of mold, g	4253.0	4253.0	4253.0	4253.0	4253.0
Mass of soil in mold, M _T	1677.4	1737.0	1771.0	1719.0	1652.0
Wet Unit Weight, γ_{wet} (kN/m ³)	17.34	17.96	18.31	17.77	17.08
Dry Unit Weight, γ_{dry} (kN/m ³)	14.20	14.42	14.30	13.31	12.10

Table B- 8 Standard compaction data for Fill 8

Standard Proctor Test (Fill 8)				
Mold Dimensions				
Height	11.7	cm	Diameter	10.2 cm
Volume	956.0401	cm ³		
Mass of Mold	4253	g		
Sample Label	1	2	3	4
Mass of cup, g	1.0	41.4	41.6	41.6
Mass of cup + wet soil, g	30.7	1867.9	1952.0	1864.3
Mass of cup + dry soil, g	24.1	1511.5	1636.7	1615.2
Mass of water, g	6.69	356.31	315.3	249.13
Mass of dry soil, g	23.07	1470.16	1595.14	1573.65
Water content, w (%)	29.00%	24.24%	19.77%	15.83%
Assumed Water Content	29%	24%	20%	16%
Water content, w (%)	29.00%	24.24%	19.77%	15.83%
Mass of soil + mold, g	5968.4	6092.0	6174.0	6088.0
Mass of mold, g	4253.0	4253.0	4253.0	4253.0
Mass of soil in mold, M _T	1715.4	1839.0	1921.0	1835.0
Wet Unit Weight, γ_{wet} (kN/m ³)	17.73	19.01	19.86	18.97
Dry Unit Weight, γ_{dry} (kN/m ³)	13.75	15.30	16.58	16.38
Dry Density ρ_{dry} , g/cm ³)	1.40	1.56	1.69	1.67

Table B- 9 Standard compaction data for Fill 10

Standard Proctor Test (Fill 10)			
Mold Dimensions			
Height	11.7	cm	Diameter 10.2 cm
Volume	956.0401	cm ³	
Mass of Mold	4253	g	
Sample Label	1	2	3
Mass of cup, g	42.1	41.6	41.6
Mass of cup + wet soil, g	1795.0	1820.0	1748.0
Mass of cup + dry soil, g	1359.9	1457.7	1440.6
Mass of water, g	435.12	362.32	307.45
Mass of dry soil, g	1317.81	1416.11	1399
Water content, w (%)	33.02%	25.59%	21.98%
Assumed Water Content	33%	26%	22%
Water content, w (%)	33.02%	25.59%	21.98%
Mass of soil + mold, g	5998.0	6036.0	5965.0
Mass of mold, g	4253.0	4253.0	4253.0
Mass of soil in mold, M _T	1745.0	1783.0	1712.0
Wet Unit Weight, γ_{wet} (kN/m ³)	18.04	18.43	17.70
Dry Unit Weight, γ_{dry} (kN/m ³)	13.56	14.68	14.51
Dry Density ρ_{dry} , g/cm ³	1.38	1.50	1.48

Table B- 10 Modified Compaction Data for Fill 6

Modified Proctor Test (Fill 6)			
Mold Dimensions			
Height	11.7	cm	Diameter 10.2 cm
Volume	956.0401	cm ³	
Mass of Mold	4268	g	
Sample Label	1	2	3
Mass of cup, g	41.5	41.6	41.6
Mass of cup + wet soil, g	1460.0	1362.0	1521.0
Mass of cup + dry soil, g	1150.0	1142.0	1318.0
Mass of water, g	310	220	203
Mass of dry soil, g	1108.47	1100.43	1276.36
Water content, w (%)	27.97%	19.99%	15.90%
Assumed Water Content	28%	20%	16%
Water content, w (%)	27.97%	19.99%	15.90%
Mass of soil + mold, g	6090.0	6154.0	6084.0
Mass of mold, g	4268.0	4268.0	4268.0
Mass of soil in mold, M _T	1822.0	1886.0	1816.0
Wet Unit Weight, γ_{wet} (kN/m ³)	18.69	19.35	18.63
Dry Unit Weight, γ_{dry} (kN/m ³)	14.61	16.12	16.07
Dry Density ρ_{dry} , g/cm ³	1.49	1.64	1.64

Table B- 11 36 kPa CU triaxial test data

Ao (m ²)	Lo (cm)	Cell Press. (kPa)	σ_3 (kPa)	Back Press. (kPa)	PWP (0 V)	Load Cell (0 V)	LVDT (Lo) (V)	
0.00417	10.59	186	35.11	150.9	0.0519	6.20	-5.051	
TIME (s)	Δ Volume(V)	PWP (V)	Load Cell (V)	LVDT (V)	Δ Volume(cc)	PWP (kPa)	Load Cell (kg)	LVDT (cm)
0	2.638	2.266	6.199	-5.050	105.361	0.000	0.000	0.000
200	2.643	2.440	6.091	-4.846	105.560	11.815	27.735	0.052
400	2.648	2.458	6.042	-4.631	105.752	13.048	40.435	0.106
600	2.653	2.431	6.008	-4.415	105.944	11.181	49.055	0.160
643	2.654	2.422	6.002	-4.369	105.987	10.595	50.518	0.172
800	2.657	2.386	5.984	-4.199	106.115	8.163	55.161	0.214
1000	2.661	2.338	5.966	-3.982	106.255	4.885	59.857	0.269
1200	2.664	2.296	5.958	-3.763	106.375	2.044	61.883	0.324

Table B- 12 72 kPa CU triaxial test data

Ao (m ²)	Lo (cm)	Cell Press. (kPa)	σ_3 (kPa)	Back Press. (kPa)	PWP (0V)	Load Cell (0V)	LVDT (Lo) (V)	
0.00420	10.61	197	72.71	124.3	0.1007	6.22	-4.462	
TIME (s)	Δ Volume(V)	PWP (V)	Load Cell (V)	LVDT (V)	Δ Volume(cc)	PWP (kPa)	Load Cell (kg)	LVDT (cm)
0	2.430	1.925	6.198	-4.461	97.058	0.000	4.669	0.000
200	2.423	2.376	6.007	-4.207	96.770	30.730	53.519	0.064
400	2.421	2.376	5.937	-3.934	96.695	30.717	71.684	0.133
570	2.426	2.326	5.902	-3.698	96.870	27.317	80.638	0.192
600	2.427	2.302	5.898	-3.657	96.910	26.656	81.665	0.202
800	2.438	2.253	5.874	-3.377	97.354	22.329	87.822	0.273
1000	2.452	2.198	5.857	-3.097	97.933	18.629	92.030	0.343
1200	2.470	2.160	5.845	-2.816	98.627	16.012	95.263	0.414

Table B- 13 144 kPa CU triaxial test data

Ao (m ²)	Lo (cm)	Cell Press. (kPa)	σ_3 (kPa)	Back Press. (kPa)	PWP (0V)	Load Cell (0V)	LVDT (Lo) (V)	
0.00416	10.69	394	148.58	245.4	0.1299	6.22	-5.390	
TIME (s)	Δ Volume(V)	PWP (V)	Load Cell (V)	LVDT (V)	Δ Volume(cc)	PWP (kPa)	Load Cell (kg)	LVDT (cm)
0	2.781	3.732	6.210	-4.830	111.051	0.000	0.359	0.000
400	2.787	4.769	5.872	-4.349	111.299	70.645	87.104	0.121
800	2.790	4.758	5.799	-3.814	11.407	69.937	105.936	0.256
1200	2.790	4.695	5.762	-3.274	11.415	65.658	115.249	0.392
1600	2.790	4.638	5.734	-2.727	111.399	61.740	122.612	0.529
1621	2.790	4.638	5.732	-2.698	111.407	61.753	123.126	0.536
2000	2.788	4.590	5.709	-2.178	111.355	58.503	128.873	0.667
2400	2.785	4.550	5.688	-1.629	111.223	55.730	134.312	0.805

Table B- 14 Fill 6 consolidation data for hydraulic conductivity

Time Rate of Consolidation Calculations							
Load =	0.12528	tsf					
H _o =	1	in					
H _s =	0.513217	in					
Time (min)	δ (in)	Δδ (in)	ε (%)	Sqrt Time (min) ^{1/2}	Ht (in)	Hv (in)	e
0.00	1.293532	0	0.00%	0.00	1	0.486783	0.948494
0.02	1.293456	7.62E-05	0.01%	0.13	0.999924	0.486707	0.948345
0.10	1.292382	0.00115	0.11%	0.32	0.999924	0.486707	0.948345
0.25	1.291175	0.002357	0.24%	0.50	0.998716	0.4855	0.945993
0.50	1.29047	0.003062	0.31%	0.71	0.998012	0.484795	0.94462
1	1.290136	0.003396	0.34%	1.00	0.997678	0.484461	0.943969
2	1.28993	0.003602	0.36%	1.41	0.997472	0.484255	0.943567
4	1.289732	0.0038	0.38%	2.00	0.997274	0.484057	0.943182
8	1.2895	0.004032	0.40%	2.83	0.997042	0.483825	0.942729
					Have =	0.9984	
					Obtain t50 and t90 from Plot of sqrt (time)		
					t90 =	0.5184	min
					t50 =	0.13	min
					The Time Factor from Table 9-1, Holtz and Kovacs		
					T90 =	0.848	
					T50 =	0.197	
					Calculations of Cv:		
					cv90 =	0.407683	in ² /min
					cv50 =	0.377672	in ² /min
					cv-ave =	0.392677	in ² /min
						1489.03	ft ² /yr
						1379.417	ft ² /yr
						1434.224	ft ² /yr

Table B- 15 Fill 8 consolidation data for hydraulic conductivity

Time Rate of Consolidation Calculations							
Load =	0.125313	tsf					
H _o =	1	in					
H _s =	0.51905	in					
Time (min)	δ (in)	Δδ (in)	ε (%)	Sqrt Time (min) ^{1/2}	Ht (in)	Hv (in)	e
0.00	1.188	0	0.00%	0.00	1	0.48095	0.926597
0.25	1.185	0.00221	0.22%	0.50	0.99779	0.47874	0.922339
0.50	1.184	0.003373	0.34%	0.71	0.996627	0.477577	0.920098
1	1.184	0.004043	0.40%	1.00	0.995957	0.476907	0.918808
2	1.183	0.004303	0.43%	1.41	0.995697	0.476647	0.918307
4	1.183	0.004483	0.45%	2.00	0.995517	0.476467	0.91796
8	1.183	0.004663	0.47%	2.83	0.995337	0.476287	0.917613
16	1.183	0.004829	0.48%	4.00	0.995171	0.476121	0.917293
					Have =	0.9965	
<i>Obtain t50 and t90 from Plot of sqrt (time)</i>							
				t90 =	0.94	min	
				t50 =	0.26	min	
<i>The Time Factor from Table 9-1, Holtz and Kovacs</i>							
				T90 =	0.848		
				T50 =	0.197		
<i>Calculations of Cv:</i>							
				cv90 =	0.223747	in ² /min	817.2189 ft ² /yr
				cv50 =	0.188104	in ² /min	687.0351 ft ² /yr
				cv-ave =	0.205926	in ² /min	752.127 ft ² /yr

Table B- 16 Fill 10 consolidation data for hydraulic conductivity

Time Rate of Consolidation Calculations							
Load =	0.125313	tsf					
H _o =	1	in					
H _s =	0.553889	in					
Time (min)	δ (in)	Δδ (in)	ε (%)	Sqrt Time (min) ^{1/2}	Ht (in)	Hv (in)	e
0.00	1.179688	0	0.00%	0.00	1	0.446111	0.805414
0.25	1.175869	0.003819	0.38%	0.50	0.996181	0.442292	0.79852
0.50	1.174508	0.00518	0.52%	0.71	0.99482	0.440931	0.796062
1	1.173862	0.005826	0.58%	1.00	0.994174	0.440285	0.794896
2	1.173541	0.006147	0.61%	1.41	0.993853	0.439964	0.794317
4	1.173288	0.0064	0.64%	2.00	0.9936	0.439711	0.79386
8	1.172936	0.006752	0.68%	2.83	0.993248	0.439359	0.793224
15	1.172753	0.006935	0.69%	3.87	0.993065	0.439176	0.792894
					Have =	0.9949	
					Obtain t₅₀ and t₉₀ from Plot of sqrt (time)		
					t ₉₀ =	0.7569	min
					t ₅₀ =	0.2	min
					The Time Factor from Table 9-1, Holtz and Kovacs		
					T ₉₀ =	0.848	
					T ₅₀ =	0.197	
					Calculations of Cv:		
					cv ₉₀ =	0.277222	in ² /min
					cv ₅₀ =	0.243729	in ² /min
					cv-ave =	0.260475	in ² /min
						1012.532	ft ² /yr
						890.2004	ft ² /yr
						951.3664	ft ² /yr

Table B- 17 Fill 10 1D Swell Test

Swell Test	
Initial Diameter of Soil	6.3246 cm
Initial Height of Soil (Ho)	2.53619 cm
Change in Height (ΔH)	0.001574 cm
Heave (%) with seating load	6.2%
Wt of Container	144.58 g
Wt of Container +Soil Wet	244.9 g
Wt of Container + Soil Dry	222.62 g
Wt Soil Dry	78.04 g
Wt Water	22.28 g
Water Content	29%
Mass of Ring	70.24 g
Start @ 8:30 AM 6/10/10	
Water @ 8:37 AM	
Took Out @ 8:54 AM 6/14/10	
AIR DRY Moisture Content Test	
Wt Container	109.82 g
Wt Container + Soil Wet	262.12 g
After Air Dry	
Wt Container + (Air Dry) Soil (48 hrs)	240.91 g
Wt Container + (Air Dry) Soil (72 hrs)	237.13 g
Wt Container + (Air Dry) Soil (96 hrs)	235.5 g
OVEN	
Final Diameter	6.19 cm
Final Height	2.522 cm

Table B- 18 Fill 6 Free Swell Test

Free Swell Test	
Initial Height of Soil (Ho)	1.1 in
Start @ 8:30 AM 2/11/11	
End @ 12:20 PM 2/12/11	
Final Height	1.27 in
Change in Height	0.17 in

APPENDIX CD: Slope/W and Vadose/W Modeling Results

Table CD- 4 Factor of safety results for 40 m high fill at 1H:1V slope

Slope Height (m)	Spacing	Slope Ratio	Month	Year	Lowest FS	Day	Slip Circle #	Slope Height (m)	Spacing	Slope Ratio	Month	Year	Lowest FS	Day	Slip Circle #	Slope Height (m)	Spacing	Slope Ratio	Month	Year	Lowest FS	Day	Slip Circle #
40	25ft	1to1	April	2009	0.627	1	12142	40	75ft	1to1	April	2009	0.634	1	11279	40	None	1to1	April	2009	0.634	1	11279
40	25ft	1to1	April	2009	0.657	2	12184	40	75ft	1to1	April	2009	0.658	2	12057	40	None	1to1	April	2009	0.658	2	12057
40	25ft	1to1	April	2009	0.644	3	10670	40	75ft	1to1	April	2009	0.631	3	12122	40	None	1to1	April	2009	0.631	3	12122
40	25ft	1to1	April	2009	0.623	4	12121	40	75ft	1to1	April	2009	0.627	4	11573	40	None	1to1	April	2009	0.627	4	11573
40	25ft	1to1	April	2009	0.643	5	12184	40	75ft	1to1	April	2009	0.657	5	12247	40	None	1to1	April	2009	0.657	5	12247
40	25ft	1to1	April	2009	0.655	6	12627	40	75ft	1to1	April	2009	0.661	6	12627	40	None	1to1	April	2009	0.661	6	12627
40	25ft	1to1	April	2009	0.65	7	12122	40	75ft	1to1	April	2009	0.661	7	12627	40	None	1to1	April	2009	0.661	7	12627
40	25ft	1to1	April	2009	0.655	8	12627	40	75ft	1to1	April	2009	0.661	8	12627	40	None	1to1	April	2009	0.661	8	12627
40	25ft	1to1	April	2009	0.661	9	11636	40	75ft	1to1	April	2009	0.661	9	12627	40	None	1to1	April	2009	0.661	9	12627
40	25ft	1to1	April	2009	0.661	10	11636	40	75ft	1to1	April	2009	0.662	10	12627	40	None	1to1	April	2009	0.662	10	12627
40	25ft	1to1	April	2009	0.661	11	11636	40	75ft	1to1	April	2009	0.654	11	12100	40	None	1to1	April	2009	0.654	11	12100
40	25ft	1to1	April	2009	0.661	12	11636	40	75ft	1to1	April	2009	0.663	12	12627	40	None	1to1	April	2009	0.663	12	12627
40	25ft	1to1	April	2009	0.661	13	11636	40	75ft	1to1	April	2009	0.647	13	12226	40	None	1to1	April	2009	0.647	13	12226
40	25ft	1to1	April	2009	0.661	14	11636	40	75ft	1to1	April	2009	0.647	14	12226	40	None	1to1	April	2009	0.647	14	12226
40	25ft	1to1	April	2009	0.661	15	11636	40	75ft	1to1	April	2009	0.647	15	12226	40	None	1to1	April	2009	0.647	15	12226
40	25ft	1to1	April	2009	0.648	16	12226	40	75ft	1to1	April	2009	0.664	16	12627	40	None	1to1	April	2009	0.664	16	12627
40	25ft	1to1	April	2009	0.653	17	12226	40	75ft	1to1	April	2009	0.664	17	12627	40	None	1to1	April	2009	0.664	17	12627
40	25ft	1to1	April	2009	0.648	18	12226	40	75ft	1to1	April	2009	0.664	18	12627	40	None	1to1	April	2009	0.664	18	12627
40	25ft	1to1	April	2009	0.622	19	12100	40	75ft	1to1	April	2009	0.665	19	12627	40	None	1to1	April	2009	0.665	19	12627
40	25ft	1to1	April	2009	0.644	20	12143	40	75ft	1to1	April	2009	0.644	20	12143	40	None	1to1	April	2009	0.644	20	12143
40	25ft	1to1	April	2009	0.635	21	12163	40	75ft	1to1	April	2009	0.649	21	12226	40	None	1to1	April	2009	0.649	21	12226
40	25ft	1to1	April	2009	0.658	22	12163	40	75ft	1to1	April	2009	0.666	22	12309	40	None	1to1	April	2009	0.666	22	12309
40	25ft	1to1	April	2009	0.658	23	12163	40	75ft	1to1	April	2009	0.666	23	12309	40	None	1to1	April	2009	0.666	23	12309
40	25ft	1to1	April	2009	0.658	24	12163	40	75ft	1to1	April	2009	0.666	24	12309	40	None	1to1	April	2009	0.666	24	12309
40	25ft	1to1	April	2009	0.658	25	12163	40	75ft	1to1	April	2009	0.659	25	12164	40	None	1to1	April	2009	0.659	25	12164
40	25ft	1to1	April	2009	0.658	26	12163	40	75ft	1to1	April	2009	0.666	26	12309	40	None	1to1	April	2009	0.666	26	12309
40	25ft	1to1	April	2009	0.658	27	12163	40	75ft	1to1	April	2009	0.666	27	12309	40	None	1to1	April	2009	0.666	27	12309
40	25ft	1to1	April	2009	0.658	28	12163	40	75ft	1to1	April	2009	0.666	28	12309	40	None	1to1	April	2009	0.666	28	12309
40	25ft	1to1	April	2009	0.658	29	12163	40	75ft	1to1	April	2009	0.666	29	12309	40	None	1to1	April	2009	0.666	29	12309
40	25ft	1to1	April	2009	0.658	30	12163	40	75ft	1to1	April	2009	0.666	30	12309	40	None	1to1	April	2009	0.666	30	12309
Slope Height (m)	Spacing	Slope Ratio	Month	Year	Lowest FS	Day	Slip Circle #	Slope Height (m)	Spacing	Slope Ratio	Month	Year	Lowest FS	Day	Slip Circle #	Slope Height (m)	Spacing	Slope Ratio	Month	Year	Lowest FS	Day	Slip Circle #
40	25ft	1to1	January	2008	0.145	1	632	40	75ft	1to1	January	2008	0.145	1	632	40	None	1to1	January	2008	0.145	1	632
40	25ft	1to1	January	2008	0.112	2	1178	40	75ft	1to1	January	2008	0.112	2	1178	40	None	1to1	January	2008	0.112	2	1178
40	25ft	1to1	January	2008	0.111	3	1178	40	75ft	1to1	January	2008	0.111	3	1178	40	None	1to1	January	2008	0.111	3	1178
40	25ft	1to1	January	2008	0.11	4	1178	40	75ft	1to1	January	2008	0.109	4	1178	40	None	1to1	January	2008	0.109	4	1178
40	25ft	1to1	January	2008	0.523	5	7060	40	75ft	1to1	January	2008	0.523	5	7060	40	None	1to1	January	2008	0.523	5	7060
40	25ft	1to1	January	2008	0.522	6	7081	40	75ft	1to1	January	2008	0.522	6	7081	40	None	1to1	January	2008	0.522	6	7081
40	25ft	1to1	January	2008	0.489	7	8402	40	75ft	1to1	January	2008	0.489	7	8402	40	None	1to1	January	2008	0.489	7	8402
40	25ft	1to1	January	2008	0.48	8	8486	40	75ft	1to1	January	2008	0.48	8	8486	40	None	1to1	January	2008	0.48	8	8486
40	25ft	1to1	January	2008	0.479	9	8486	40	75ft	1to1	January	2008	0.479	9	8486	40	None	1to1	January	2008	0.479	9	8486
40	25ft	1to1	January	2008	0.475	10	8549	40	75ft	1to1	January	2008	0.475	10	8549	40	None	1to1	January	2008	0.475	10	8549
40	25ft	1to1	January	2008	0.473	11	8654	40	75ft	1to1	January	2008	0.473	11	8654	40	None	1to1	January	2008	0.473	11	8654
40	25ft	1to1	January	2008	0.581	12	6408	40	75ft	1to1	January	2008	0.581	12	6408	40	None	1to1	January	2008	0.581	12	6408
40	25ft	1to1	January	2008	0.583	13	6408	40	75ft	1to1	January	2008	0.583	13	6408	40	None	1to1	January	2008	0.583	13	6408
40	25ft	1to1	January	2008	0.584	14	6408	40	75ft	1to1	January	2008	0.584	14	6408	40	None	1to1	January	2008	0.584	14	6408
40	25ft	1to1	January	2008	0.585	15	6408	40	75ft	1to1	January	2008	0.585	15	6408	40	None	1to1	January	2008	0.585	15	6408
40	25ft	1to1	January	2008	0.585	16	6513	40	75ft	1to1	January	2008	0.584	16	6513	40	None	1to1	January	2008	0.584	16	6513
40	25ft	1to1	January	2008	0.585	17	6513	40	75ft	1to1	January	2008	0.585	17	6513	40	None	1to1	January	2008	0.585	17	6513
40	25ft	1to1	January	2008	0.586	18	6513	40	75ft	1to1	January	2008	0.586	18	6513	40	None	1to1	January	2008	0.586	18	6513
40	25ft	1to1	January	2008	0.586	19	6513	40	75ft	1to1	January	2008	0.586	19	6513	40	None	1to1	January	2008	0.586	19	6513
40	25ft	1to1	January	2008	0.587	20	6513	40	75ft	1to1	January	2008	0.587	20	6513	40	None	1to1	January	2008	0.587	20	6513
40	25ft	1to1	January	2008	0.587	21	6513	40	75ft	1to1	January	2008	0.587	21	6513	40	None	1to1	January	2008	0.587	21	6513
40	25ft	1to1	January	2008	0.587	22	6513	40	75ft	1to1	January	2008	0.587	22	6513	40	None	1to1	January	2008	0.587	22	6513
40	25ft	1to1	January	2008	0.588	23	6513	40	75ft	1to1	January	2008	0.588	23	6513	40	None	1to1	January	2008	0.588	23	6513
40	25ft	1to1	January	2008	0.58	24	12121	40	75ft	1to1	January	2008	0.584	24	12100	40	None	1to1	January	2008	0.584	24	12100
40	25ft	1to1	January	2008	0.591	25	6513	40	75ft	1to1	January	2008	0.591	25	6513	40	None	1to1	January	2008	0.591	25	6513
40	25ft	1to1	January	2008	0.592	26	6492	40	75ft	1to1	January	2008	0.592	26	6492	40	None	1to1	January	2008	0.592	26	6492
40	25ft	1to1	January	2008	0.593	27	6492	40	75ft	1to1	January	2008	0.593	27	6492	40	None	1to1	January	2008	0.593	27	6492
40	25ft	1to1	January	2008	0.593	28	6492	40	75ft	1to1	January	2008	0.593	28	6492	40	None	1to1	January	2008	0.593	28	6492
40	25ft	1to1	January	2008	0.593	29	6492	40	75ft	1to1	January	2008	0.59	29	12121	40	None	1to1	January	2008	0.59	29	12121
40	25ft	1to1	January	2008	0.593	30	6492	40	75ft	2to1	January	2008	0.593	30	6492	40	None	2to1	January	2008	0.593	30	6492
40	25ft	1to1	January	2008	0.592	31	6492	40	75ft	2to1	January	2008</											

THIS PAGE INTENTIONALLY LEFT BLANK